



HAL
open science

An EWMA sign chart for dispersion with exact run length properties

Theodoros Perdikis, Stelios Psarakis, Philippe Castagliola, Vicent Giner-Bosch, Petros E Maravelakis, Athanasios C Rakitzis

► **To cite this version:**

Theodoros Perdikis, Stelios Psarakis, Philippe Castagliola, Vicent Giner-Bosch, Petros E Maravelakis, et al.. An EWMA sign chart for dispersion with exact run length properties. *Journal of Statistical Computation and Simulation*, 2023, 93 (11), pp.1799-1829. 10.1080/00949655.2022.2154767 . hal-04141744

HAL Id: hal-04141744

<https://hal.science/hal-04141744>

Submitted on 26 Jun 2023

HAL is a multi-disciplinary open access archive for the deposit and dissemination of scientific research documents, whether they are published or not. The documents may come from teaching and research institutions in France or abroad, or from public or private research centers.

L'archive ouverte pluridisciplinaire **HAL**, est destinée au dépôt et à la diffusion de documents scientifiques de niveau recherche, publiés ou non, émanant des établissements d'enseignement et de recherche français ou étrangers, des laboratoires publics ou privés.

An EWMA Sign Chart for dispersion with exact Run Length properties

Theodoros. Perdikis^a and Stelios Psarakis^a and Philippe Castagliola^b and Vicent Giner-Bosch^c and Petros E. Maravelakis^d and Athanasios C. Rakitzis^e

^aDepartment of Statistics & Laboratory of Statistical Methodology, Athens University of Economics and Business, Athens, Greece; ^bNantes Université & LS2N UMR CNRS 6004, Nantes, France; ^cCentre for Quality and Change Management, Universitat Politècnica de València, Spain; ^d Department of Business Administration, University of Piraeus, Piraeus, Greece; ^e Department of Statistics and Insurance Science, University of Piraeus, Piraeus, Greece

ARTICLE HISTORY

Compiled June 26, 2023

ABSTRACT

The EWMA Sign control chart is a distribution-free scheme used for monitoring shifts in the location parameter during process monitoring. In this work, we propose a modified Phase II EWMA chart based on a general Sign statistic, capable of monitoring shifts in the process variability. Regarding the determination of the proposed chart's in- and out-of-control Run Length properties, Markov chain methods are used in combination with a continuous transformation of the suggested general Sign statistic. Our results show the power of the proposed method regarding the proposed chart's *exact* Run Length properties and its efficiency in detecting shifts in the process variability.

KEYWORDS

distribution-free; Sign statistic; Markov chain; EWMA control chart; variability

1. Introduction

Control charts have been widely used in manufacturing industries, as a powerful tool for the on-line monitoring of a process. Shewhart [1] is considered as the pioneer of control charts, introducing schemes capable of monitoring relative large shifts in the process mean (\bar{X} chart) or the variability (R and S charts). Additionally, when shifts of small magnitude occur in the process parameters, Cumulative Sum (CUSUM, see Page in [2]) or Exponentially Weighted Moving Average (EWMA, see Roberts in [3]) charts are preferable due to their superiority in early shift detection. In general, in the design of conventional control charts as the ones mentioned above, it is assumed that the distribution of the observations collected over time is known, with the most common choice being that of normal distribution. However, in practice, either the assumption of, say, normal distribution is violated or practitioners do not want to use a specific distribution model for their process. As a result, designing schemes capable of monitoring shifts in the process without any knowledge of the

observations' underlying distribution, has drawn the researchers' attention and led to nonparametric (or distribution-free) control charts. In particular, with regard to monitoring process location, nonparametric tests such as the Sign Test are used for detecting shifts in the process median without the knowledge of the distribution of the quality characteristic of interest (see, [4], [5], [6], [7], [8], [9], [10]). Similarly, several nonparametric control charts have been introduced in the literature for detecting shifts in the process variability, such as Shewhart-type (see, [11], [12], [13], [14]) or EWMA and CUSUM schemes (see, [15], [16], [17], [18], [19]). For a comprehensive overview of existing univariate and multivariate nonparametric control charts the reader is advised to refer to [20] and [21].

With respect to the design of a phase II control chart, for Shewhart-type schemes, their Run Length (RL) properties, such as the Average Run Length (ARL) and the Standard Deviation Run Length (SDRL), are obtained by assuming that the random variable RL follows a geometric distribution. On the other hand, for EWMA and CUSUM-type schemes, their RL properties are usually computed using the Markov chain method of Brook and Evans in [22]. However, as recent studies have shown (see, Wu et al. in [23] and Perdikis et al. in [24]), the method of Brook and Evans [22] does not always provide a reliable approximation of the RL properties of a nonparametric EWMA or CUSUM control chart. More specifically, due to the discrete nature of the statistics whose values are monitored (for example the sign statistic), the method of Brook and Evans [22] leads to unreliable results regarding the chart's in-control and out-of-control ARL values. As a solution to this problem, Castagliola et al. in [25], following the approach of Rakitzis et al. in [26]), proposed an EWMA-type scheme (denoted as the CEWMA SN chart) in which the charting statistic, at each sampling point is an integer, and by adding some simple modifications in the Markov chain method, it was possible to determine the *exact* in- and out-of-control ARL values. Additional studies based on the approach of Castagliola et al. (2019) in [25] can also be found in [27] and [28]. Recently, Wu et al. in [23], proposed a new method, in which the initial discrete random variable to be monitored is turned into a continuous one, as a mixture of normally distributed random variables. Based on their findings, their proposed method, yields steady ARL values and it guarantees a reliable and accurate approximation of chart's RL properties.

In this work, we aim to present a new nonparametric control chart for monitoring the process variability. In particular, a generalization of the charting statistic used by Amin et al. in [11] will be introduced for the design of the proposed scheme and detailed guidelines to practitioners will be given regarding the chart's optimal design parameters. Additionally, we will provide a methodology that will guarantee the chart's exact RL properties. More specifically, as it will be proven in the following sections, the proposed control chart is distribution-free meaning that its statistical design does not require any knowledge about the underlying distribution and it has reliable and steady ARL values.

This paper is organised as follows: In Section 2, a brief review on the theoretical properties of the nonparametric Shewhart chart, introduced by Amin et al. in [11], based on the Sign-type statistic for dispersion is presented and a general version of this statistic is suggested. Additionally, in Section 3, a modified EWMA chart based on the Sign statistic for monitoring shifts in the process variability is introduced and in Section 4, the efficiency of the method of Brook and Evans [22] is tested for the compu-

tation of the proposed chart's RL properties. In Section 5, a Kernel-based methodology is used in order to improve the proposed chart's in- and out-of-control RL properties. Moreover, in Section 6, the out-of-control performance of the proposed chart is investigated and its performance is compared with other schemes for monitoring process variability. Finally, in Section 7 an illustrative example is provided while in Section 8 conclusions along with suggestions for future research work are given.

2. The Interquantile Range Sign statistic for dispersion

Suppose that, at each sampling point t , a random sample $\{X_{t,1}, X_{t,2}, \dots, X_{t,n}\}$ of size n is collected, where $X_{t,j}$, $j = 1, 2, \dots, n$, follows an unknown continuous distribution with corresponding cumulative distribution function (c.d.f.) $F_X(x|\sigma)$. The parameter σ corresponds to the standard deviation of the distribution, that is the parameter of interest. It is assumed that $\sigma = \sigma_0$ when the process is in-control and $\sigma = \sigma_1 = \tau\sigma_0$ when the process is out-of-control. The parameter τ reflects the shift magnitude in the process variability, i.e. $\tau \in (0, 1)$ corresponds to a decrease in the variability (usually associated to a process improvement) while $\tau \in (1, +\infty)$ corresponds to an increase in the variability (usually associated to a process deterioration).

Let $X_{p_0/2}$ and $X_{1-p_0/2}$ be the $p_0/2$ and $1 - p_0/2$ quantiles of $F_X(x|\sigma_0)$, i.e. when the process is *in-control*, where $p_0 \in (0, 1)$ is a parameter considered to be known (or pre-specified). By definition, $X_{p_0/2}$ and $X_{1-p_0/2}$ are such that $F_X(X_{p_0/2}|\sigma_0) = p_0/2$, $F_X(X_{1-p_0/2}|\sigma_0) = 1 - p_0/2$ and we directly deduce that

$$p_0 = 1 - F_X(X_{1-p_0/2}|\sigma_0) + F_X(X_{p_0/2}|\sigma_0).$$

When the process shifts from σ_0 to σ_1 , the corresponding probability is defined as

$$p_1 = 1 - F_X(X_{1-p_0/2}|\sigma_1) + F_X(X_{p_0/2}|\sigma_1).$$

If $\sigma_1 < \sigma_0$ (decrease in the variability) then we have $p_1 < p_0$ and if $\sigma_1 > \sigma_0$ (increase in the variability) then we have $p_1 > p_0$. Consequently, a shift from σ_0 to σ_1 in one direction is similar to a shift from p_0 to p_1 in the same direction. This suggests a simple distribution-free Shewhart-type Sign chart for monitoring shifts in the process variability based on the following statistic

$$SD_t = \sum_{j=1}^n D_{t,j},$$

where

$$D_{t,j} = \begin{cases} 1, & \text{if } X_{t,j} < X_{p_0/2} \text{ or } X_{t,j} > X_{1-p_0/2} \\ 0, & \text{if } X_{t,j} = X_{p_0/2} \text{ or } X_{t,j} = X_{1-p_0/2} \\ -1, & \text{if } X_{p_0/2} < X_{t,j} < X_{1-p_0/2} \end{cases}.$$

Note that, due to the continuous nature of the variables to be monitored, the condition $D_{t,j} = 0$ is not supposed to hold in practice. Similarly with the theoretical properties of the traditional Sign statistic for testing changes in the median, the SD_t

statistic belongs to $\{-n, -n + 2, \dots, n - 2, n\}$. In addition, let us define the random variable $A_t = \frac{SD_t + n}{2}$ as the number of observations less than $X_{p_0/2}$ or larger than $X_{1-p_0/2}$. By definition, this random variable A_t follows a binomial distribution $\text{Bin}(n, p)$ with parameters n and $p \in \{p_0, p_1\}$ (depending on whether the process is in- or out-of-control). Therefore, we obtain the c.d.f. $F_{SD_t}(s|n, p)$ of SD_t with the help of the c.d.f. $F_{\text{Bin}}(\cdot|n, p)$ of the $\text{Bin}(n, p)$ as

$$F_{SD_t}(s|n, p) = F_{\text{Bin}}\left(\frac{s + n}{2}|n, p\right), s \in \{-n, -n + 2, \dots, n - 2, n\}.$$

In addition, the mean $E(SD_t)$ and the variance $V(SD_t)$ are given by

$$E(SD_t) = 2E(A_t) - n = n(2p - 1), \quad (1)$$

$$V(SD_t) = 4V(A_t) = 4np(1 - p). \quad (2)$$

In general, in existing works related with nonparametric Shewhart schemes based on the Interquantile Range Sign statistic ([11]), a fixed value of $p_0 = 0.5$ has been considered regardless of the shift magnitude to be detected. Pawar et al. in [29] proposed a nonparametric upper-sided Shewhart chart for dispersion, based on the SD_t statistic where the value of p_0 is allowed to vary. During the design phase of their scheme, for different values of p_0 , they examined the chart's out-of-control performance. Note that, Pawar et al. [29] only considered values of $\tau > 1$ (i.e., the case of increasing shifts in process variability). In this work, we aim to introduce an EWMA chart based on the SD_t statistic and investigate the optimal value of p_0 for efficiently monitoring a process and detecting a specific shift (increase or decrease) of magnitude τ in the in-control variability σ_0 .

3. The D-SN EWMA chart for dispersion

The nonparametric EWMA chart based on the Sign statistic was originally introduced by Graham et al. in [5] as a control scheme capable of detecting shifts in the process median. Using the Markov chain approach of Brook and Evans in [22], they computed its optimal design parameters and presented its out-of-control performance under different continuous distributions. In this work, we will present an extended version of the Sign EWMA chart presented in [5] for monitoring shifts in the process variability. In particular, based on the design of the standard Sign EWMA scheme introduced in [5], instead of using the Sign statistic, we will use the SD_t statistic, previously presented in Section 2, for monitoring shifts in the process dispersion.

3.1. Charting statistic and control limits

The plotting statistic for the two-sided EWMA chart based on the SD_t statistic suggested in the previous Section (to be denoted as the D-SN EWMA chart) will be computed by the following recursive formula as:

$$Z_t = \lambda SD_t + (1 - \lambda)Z_{t-1}, Z_0 = E_0(SD_t), \quad (3)$$

with $\lambda \in (0, 1]$ and $E_0(\text{SD}_t)$ is the in-control mean of SD_t . For an indication of a shift in the process dispersion, a signal will be given if the value of the charting statistic Z_t lies outside the interval $[\text{LCL}, \text{UCL}]$ where LCL and UCL are the asymptotic (or steady-state) upper and lower control limits computed as:

$$\begin{aligned}\text{LCL} &= E_0(\text{SD}_t) - K \sqrt{V_0(\text{SD}_t)} \times \sqrt{\frac{\lambda}{2 - \lambda}}, \\ \text{UCL} &= E_0(\text{SD}_t) + K \sqrt{V_0(\text{SD}_t)} \times \sqrt{\frac{\lambda}{2 - \lambda}},\end{aligned}\tag{4}$$

where $K > 0$ is a coefficient to be fixed. When the process is in-control, the corresponding in-control mean $E_0(\text{SD}_t)$ and variance $V_0(\text{SD}_t)$ of SD_t are obtained by substituting $p = p_0$ in (1) and (2) respectively. Therefore, the control limits can be rewritten as:

$$\begin{aligned}\text{LCL} &= n(2p_0 - 1) - 2K \sqrt{\frac{\lambda n p_0 (1 - p_0)}{2 - \lambda}}, \\ \text{UCL} &= n(2p_0 - 1) + 2K \sqrt{\frac{\lambda n p_0 (1 - p_0)}{2 - \lambda}}.\end{aligned}$$

It should be clarified that the values of the quantiles $X_{p_0/2}$ and $X_{1-p_0/2}$ do not have any impact on the in-control design of the control chart. In particular, the determination of the control limits, and the pair (λ, K) only depend on the sample size n and the value of p_0 which is a value to be fixed by the practitioner (more details regarding the determination of this value are provided in the following Sections). Of course, we may argue the fact that the chart's operation during phase II requires the values of the quantiles to be known or at least estimated (during phase I), similarly to what happens with any parametric or nonparametric scheme. However, their values does not affect the chart's RL properties. Without loss of generality in the rest of this work, we assume that these quantiles are known.

3.2. RL properties

In order to obtain the RL properties of the proposed scheme, following the same design of a conventional EWMA chart (parametric or not), the ‘‘standard’’ method of Brook and Evans [22] will be used and its robustness will be investigated. In particular, it is assumed that the operation of the EWMA control chart can be well represented through a discrete-time Markov chain where the control limit interval $[\text{LCL}, \text{UCL}]$ is divided into $2m + 1$ subintervals of width 2Δ where $\Delta = \frac{\text{UCL} - \text{LCL}}{4m + 2}$. Additionally, for each transient state $j = \{-m, \dots, 0, \dots, m\}$, the corresponding j -th midpoint is defined as $H_j = \frac{\text{LCL} + \text{UCL}}{2} + 2j\Delta$. Then, the transition probability matrix \mathbf{P} for the two-sided

D-SN EWMA chart is computed as:

$$\mathbf{P} = \begin{pmatrix} \mathbf{Q} & \mathbf{r} \\ \mathbf{0}^\top & 1 \end{pmatrix} = \begin{pmatrix} Q_{-m,-m} & \cdots & Q_{-m,-1} & Q_{-m,0} & Q_{-m,1} & \cdots & Q_{-m,m} & r_{-m} \\ \vdots & \vdots & \vdots & \vdots & \vdots & \vdots & \vdots & \vdots \\ Q_{-1,-m} & \cdots & Q_{-1,-1} & Q_{-1,0} & Q_{-1,1} & \cdots & Q_{-1,m} & r_{-1} \\ Q_{0,-m} & \cdots & Q_{0,-1} & Q_{0,0} & Q_{0,1} & \cdots & Q_{0,m} & r_0 \\ Q_{1,-m} & \cdots & Q_{1,-1} & Q_{1,0} & Q_{1,1} & \cdots & Q_{1,m} & r_1 \\ \vdots & \vdots & \vdots & \vdots & \vdots & \vdots & \vdots & \vdots \\ Q_{m,-m} & \cdots & Q_{m,-1} & Q_{m,0} & Q_{m,1} & \cdots & Q_{m,m} & r_m \\ 0 & \cdots & 0 & 0 & 0 & \cdots & 0 & 1 \end{pmatrix}$$

where \mathbf{Q} is the $(2m + 1, 2m + 1)$ matrix of transient probabilities, $\mathbf{0}^\top = (0, 0, \dots, 0)$ and $\mathbf{r} = \mathbf{1} - \mathbf{Q}\mathbf{1}$. Let $\mathbf{q} = (q_{-m}, \dots, q_0, \dots, q_m)^\top$ be the $(2m + 1, 1)$ vector of initial probabilities associated with the $2m + 1$ transient states. In particular, this vector contains the probabilities that the charting statistic Z_t starts in a given state. Therefore, we use $\mathbf{q} = (0, \dots, 1, \dots, 0)^\top$ where the value 1 at the m -th entry, corresponds to $Z_0 = E_0(\text{SD}_t)$ stating that the process starts at state m . That is, the initial value for the EWMA statistic in (3) is the in-control mean of SD_t . Finally, the transient probabilities, $Q_{j,k}$ are obtained as:

$$\begin{aligned} Q_{j,k} &= P(Z_t \text{ is in state } k | Z_{t-1} \text{ is in state } j) \\ &= P(H_k - \Delta \leq Z_t \leq H_k + \Delta | Z_{t-1} = H_j). \end{aligned} \quad (5)$$

Using the definition of the charting statistic, Z_t , defined in (3), and substituting into (5), the transient probabilities, $Q_{j,k}$ are equal to:

$$\begin{aligned} Q_{j,k} &= P(H_k - \Delta \leq \lambda \text{SD}_t + (1 - \lambda)Z_{t-1} \leq H_k + \Delta | Z_{t-1} = H_j) \\ &= P\left(\frac{H_k - \Delta - (1 - \lambda)H_j}{\lambda} \leq \text{SD}_t \leq \frac{H_k + \Delta - (1 - \lambda)H_j}{\lambda}\right) \\ &= F_{\text{Bin}}\left(\frac{\frac{H_k + \Delta - (1 - \lambda)H_j}{\lambda} + n}{2} | n, p\right) - F_{\text{Bin}}\left(\frac{\frac{H_k - \Delta - (1 - \lambda)H_j}{\lambda} + n}{2} | n, p\right), \end{aligned}$$

where $p \in \{p_0, p_1\}$. It is clear that when $p = p_0$ we are referring to the in-control ARL and when $p = p_1$ we are referring to the out-of-control one.

Finally, for a sufficient large number of subintervals $2m + 1$ the ARL and SDRL values can be accurately evaluated using the following classical formulas from the Markov chain theory (see, for instance [30,31])

$$\begin{aligned} \text{ARL} &= \mathbf{q}^\top (\mathbf{I} - \mathbf{Q})^{-1} \mathbf{1}, \\ \text{SDRL} &= \sqrt{2\mathbf{q}^\top (\mathbf{I} - \mathbf{Q})^{-2} \mathbf{Q}\mathbf{1} + \text{ARL}(1 - \text{ARL})}. \end{aligned}$$

4. Numerical analysis

The investigation of the proposed chart's RL properties, will be examined under several symmetric and asymmetric distributions trying to cover a large variety of cases including heavily-tailed distributions. In particular, following the semi-parametric design presented by Castagliola et al. in [32], the robustness of the chart's RL properties will be tested under a benchmark of 18 Johnson's type distributions.

4.1. Johnson Distributions

Generally, the c.d.f. $F_Z(\dots)$ of a Johnson's-type distribution with parameters $a, b > 0$, c and $d > 0$ is defined as:

- bounded on $[c, c + d]$ (denoted as B in Table 1) with $F_Z(x)$ equal to:

$$F_Z(x) = F_N\left(a + b \ln\left(\frac{x - c}{c + d - x}\right)\right), x \in [c, c + d]$$

- unbounded on $(-\infty, \infty)$ (denoted as U in Table 1) with $F_Z(x)$ equal to:

$$F_Z(x) = F_N\left(a + b \sinh^{-1}\left(\frac{x - c}{d}\right)\right), x \in (-\infty, \infty)$$

where $F_N(\dots)$ is the c.d.f. of the standard normal distribution.

In Table 1, 18 cases of the Johnson's family distributions are presented. Moreover, for each distribution, the corresponding values of the parameters a, b, c, d , have been selected in order to satisfy $\text{med}(Z) = 0$ (for the median) and $\sigma(Z) = 1$ (for the standard-deviation). The cases #1–#6 approximately match some well known symmetric distributions. In particular, case #1 is close to the Uniform distribution, case #2 is close to the Triangular distribution while case #3 almost corresponds to the Standard Normal distribution. Additionally, cases #4–#6 are close to the Student t distribution with 10, 6 and 5 degrees of freedom, respectively. Finally, the remaining 12 cases, under different values for the skewness $\gamma_3 > 0$ and kurtosis $\gamma_4 > 0$ aim to cover a large variety of asymmetric and heavily-tailed distributions. For more details, a graphical representation of these distribution is provided page 116 in [32].

4.2. Effect of the number of subintervals

In this Section, we aim to investigate the effect of the number of subintervals in the RL properties of our proposed chart when the method of Brook and Evans [22] is being used. Generally, in cases where the statistic to be monitored is a continuous one (for instance, in parametric EWMA control charts based on the \bar{X} statistic), for a relatively large number of subintervals (say $2m + 1 \approx 201$), the method of Brook and Evans [22] provides a reliable approximation of the chart's RL properties such

Table 1.: Benchmark of 18 Johnson’s type distributions.

case	γ_3	γ_4	type	a	b	c	d
1	0	-1.2	B	0	0.64646	-1.81530	3.63060
2	0	-0.6	B	0	1.39830	-3.10970	6.21950
3	0	0	U	0	100	0	100
4	0	1	U	0	2.3212	0	2.10940
5	0	3	U	0	1.6104	0	1.31180
6	0	6	U	0	1.3493	0	1
7	2	4.3	B	1.7464	0.69076	-0.48932	6.6213
8	2	6.1	B	3.3279	1.227	-1.0016	16.088
9	2	7.9	U	-4.85600	1.8044	-1.41900	0.19332
10	2	10.8	U	-1.0444	1.432	-0.65538	0.82361
11	2	16.7	U	-0.52977	1.2093	-0.33154	0.73314
12	2	25.5	U	-0.34371	1.0892	-0.2023	0.63054
13	5	39.9	B	3.3715	0.74593	-0.27094	25.150
14	5	52.6	B	5.2193	0.98134	-0.47316	97.043
15	5	65.3	U	-4.01870	1.0864	-0.56652	0.02806
16	5	86	U	-0.75701	0.98744	-0.32033	0.37954
17	5	128.7	U	-0.43187	0.90797	-0.18538	0.37543
18	5	192.1	U	-0.29868	0.85558	-0.12122	0.34029

as the ARL or the SDRL. However, recent studies have shown that, computing the RL properties of a nonparametric EWMA chart via the “conventional” method of Brook and Evans [22] does not always guarantee an optimal design because the ARL and the SDRL values are strongly affected by the number of subintervals $2m + 1$. For instance, Wu et al. [23] investigated the design of a distribution-free EWMA chart based on a Sign-type statistic and proved that the number of subintervals $2m + 1$ significantly affects the ARL values. Additionally, Perdakis et al. [24] showed that in the design of an EWMA chart based on the Wilcoxon Signed Rank statistic, the ARL values are also affected by the number of subintervals. Based on our numerical analysis, the same behavior appears on the proposed scheme. More specifically, in Table 2(top), using the standard approach of Brook and Evans [22] the corresponding in-control ARL values are computed for different combinations of $n = \{12, 20\}$ and $p_0 = \{0.3, 0.5, 0.6, 0.8\}$. The values of $\lambda = 0.2$ and $K = 2.85$ have been chosen only for illustration purposes. From Table 2 it can be clearly concluded that, regardless the value of n or p_0 , the ARL_0 is affected by the number of subintervals instead of converging to the exact value of the ARL as the number of subintervals increases. As an example, if we take a closer look when $(n = 12, p_0 = 0.3)$ the ARL ranges from 349.6 to 395.5 while the exact ARL, value approximated through a Monte Carlo simulation of 10^5 iterations, is around 382 (see bottom row denoted “sim”).

Additionally, in Table 3 (top), using the same values for the parameters (λ, K) , the out-of-control ARL values are presented for $\tau = 1.1$, $p_0 = 0.5$ and $n = 5$ under the Benchmark of 18 Johnson’s type distributions illustrated in Table 1. Similarly, in Table 4 (top) the corresponding ARL values are presented for $\tau = 0.9$, $p_0 = 0.5$ and $n = 5$. Note that, $\tau = 1.1$ corresponds to a small increase and $\tau = 0.9$ corresponds to a small decrease in the variability. For each case, the corresponding out-of-control probabilities are computed as:

$$p_1 = 1 - F_Z(X_{1-p_0/2}|a, b, \tau c, \tau d) + F_Z(X_{p_0/2}|a, b, \tau c, \tau d) \quad (6)$$

From Tables 3 (top) and 4 (top) we may conclude that a very similar pattern also occurs for the out-of-control ARL values regardless the underlying distribution. As a result, using the standard method of Brook and Evans [22], practitioners are not

able to compute the *exact* in- and out-of-control ARL values of this chart and, as a consequence, they are not able to find a suitable pair of (λ, K) to guarantee the chart's optimal performance.

5. The D-SN-C EWMA chart for dispersion (The “continuousified” approach)

From the results presented in section 3, we noticed that the ARL values obtained with the classical method of Brook and Evans [22] may not always lead to steady results regarding the design of an EWMA chart based on the SD_t statistic. The primary goal is to design an EWMA scheme for dispersion in which the ARL values will remain unaffected by the number of subintervals. Wu et al. [23] proposed the “continuousify” method, which suggests the transformation of any discrete charting statistic into a continuous one; the transformed statistic is a mixture of weighted Normal r.v. In particular, they showed that this transformation not only improves significantly the chart's RL properties but it also enables practitioners to optimize the chart's parameters in order to achieve in-control ARL value exactly equal to the desired one (say 370.4). Recently, many authors used this method for the design of several nonparametric EWMA control charts and they proved the superiority of the “continuousify” method (see [33],[34]). As a consequence, motivated by these results in the related literature, we will use this technique for the design of our proposed chart (to be denoted as the D-SN-C EWMA chart).

Let $X_t, t = 1, 2, \dots$ be a sequence of i.i.d. discrete random variables, each of them defined on $\Psi = \{\psi_1, \psi_2, \dots\}$ with corresponding p.m.f. function $f_X(\psi|\boldsymbol{\theta})$ where $\boldsymbol{\theta}$ denotes the vector of parameters. As stated in [23], X can be transformed into a new *continuous* random variable (denoted as X_t^*), defined as a mixture of normally distributed random variables Y_t^* where, for each $\psi_t \in \Psi, Y_t^* \sim N(\psi_t, h)$. Then, the corresponding p.m.f. $f_{X^*}(x|\boldsymbol{\theta})$ and c.d.f. $F_{X^*}(x|\boldsymbol{\theta})$ of X_t^* will be computed as:

$$f_{X^*}(x|\boldsymbol{\theta}) = \sum_{\psi \in \Psi} f_X(\psi|\boldsymbol{\theta}) f_N(x|\psi, h),$$

$$F_{X^*}(x|\boldsymbol{\theta}) = \sum_{\psi \in \Psi} f_X(\psi|\boldsymbol{\theta}) F_N(x|\psi, h),$$

where $f_N(x|\psi, h)$ and $F_N(x|\psi, h)$ are the p.d.f. and c.d.f. of the Normal (ψ, h) distribution, respectively, where $h > 0$ is the “continuousified” parameter and it is a value to be fixed. For more details regarding the definition or similar applications of the “continuousify” method the reader is referred to [33],[34]. For our proposed “continuousified” two-sided Sign EWMA chart for dispersion instead of using SD_t , a new continuous statistic will be used, denoted as SD_t^* . Since the domain in which SD_t is

defined is $\Psi = \{-n, -n + 2, \dots, n - 2, n\}$, the statistic SD_t will be transformed into:

$$SD_t^* = \begin{cases} SD_{t,-n}^* \sim N(-n, h), & \text{if } SD_t = -n \\ SD_{t,-n+2}^* \sim N(-n + 2, h), & \text{if } SD_t = -n + 2 \\ \vdots & \vdots \\ SD_{t,0}^* \sim N(0, h), & \text{if } SD_t = 0 \\ \vdots & \vdots \\ SD_{t,n-2}^* \sim N(n - 2, h), & \text{if } SD_t = n - 2 \\ SD_{t,n}^* \sim N(n, h), & \text{if } SD_t = n \end{cases}.$$

Additionally, the c.d.f. $F_{SD_t^*}(s|n, p)$ of SD_t^* will be defined for $s \in \mathbb{R}$ and will be equal to

$$F_{SD_t^*}(s|n, p) = \sum_{\psi \in \Psi} f_{\text{Bin}}\left(\frac{\psi + n}{2} | n, p\right) F_N(s|\psi, h). \quad (7)$$

Finally, as for the computation of the mean and variance of SD_t^* , following the definitions of the mean and variance of a continuous random variable, it can be easily proven that (see, Appendix):

$$E(SD_t^*) = E(SD_t), \quad (8)$$

$$V(SD_t^*) = V(SD_t) + h^2 \quad (9)$$

Regarding the charting statistic of the proposed two-sided D-SN-C EWMA chart, it will be simply defined as:

$$Z_t^* = \lambda SD_t^* + (1 - \lambda) Z_{t-1}^*, Z_0^* = E_0(SD_t^*). \quad (10)$$

Lastly, in the expressions presented in (4), if we substitute the mean and variance by the equations (8) and (9), the new control limits LCL and UCL, denoted as LCL^* and UCL^* respectively, of our proposed scheme will be:

$$LCL^* = n(2p_0 - 1) - K \sqrt{\frac{\lambda(4np_0(1 - p_0) + h^2)}{2 - \lambda}}, \quad (11)$$

$$UCL^* = n(2p_0 - 1) + K \sqrt{\frac{\lambda(4np_0(1 - p_0) + h^2)}{2 - \lambda}}. \quad (12)$$

In order to verify the efficiency of the proposed chart in terms of its stability for the computation of the ARL values, in Tables 2 and 3 (bottom), besides the ARL values already obtained by the classical method of Brook and Evans [22], the corresponding ARL values obtained via the ‘‘continuousify’’ method are presented. For the in-control case (Table 2), we may conclude that, regardless the values of n and p_0 , the use of the continuous transformation in the discrete statistic to be monitored, provides a great improvement. More specifically, for every combination of (n, p_0) , the corresponding ARL values become stable really quickly even for small values of $2m + 1 \approx 51$. Similarly with the in-control cases, from Tables 3 and 4, it can be concluded that the advantages

of the “continuousify” method are also present in the out-of-control cases. In particular, for all the 18 distributions, the ARL values without the “continuousify” method are not stable and depend on the number of subintervals. On the other hand, by using the continuous transformation the ARL values become stable and seem to be unaffected by the number of subintervals. Regarding the value of the “continuousify” parameter h , as it has already been shown in [23] and [24], as soon as this parameter is not too small or not too large (say $h \approx 0.2$) the results are not seriously affected. In Table 5, for different combinations of the sample size, $n \in \{7, 13, 18, 22\}$, and a pre-specified probability, $p_0 \in \{0.4, 0.5, 0.6, 0.7, 0.8\}$, the corresponding in-control ARL values of the D-SN-C EWMA chart are presented for $h \in \{0.1, 0.15, \dots, 0.3\}$. Based on the results from Table 5 it is clear that h does not significantly affect the results as only some minor differences exist in the first decimal place for small values of $2m + 1$. As a result, setting a value of $h = 0.2$ is suggested. It should be noted that from Tables 3 and 4 we may see that the ARL values obtained with the “continuousify” method are a bit larger than those obtained by simulation. This is logical as the control limits obtained with the “continuousify” method are a bit larger than those obtained without the “continuousify” method due to the extra term h . This is the price to pay in order to obtain reliable ARL values.

6. Optimization of the D-SN-C EWMA chart

In this section we aim to investigate how the value of p_0 (i.e. the value that needs to be fixed during the design phase of the chart) affects the chart’s out-of-control performance. In particular, we will investigate the impact of varying values of p_0 (instead of being set to $p_0 = 0.5$) under different shift magnitudes and underlying distributions. In Table 6 the chart’s out-of-control performance is presented for $p_0 \in \{0.1, 0.5, 0.7\}$ for the distributions listed in Table 1. For illustration purposes the values of the design parameters are randomly selected and equal to ($\lambda = 0.2, K = 2.75, n = 10, h = 0.2$). From the results presented in Table 6 it is clear that the initial value of p_0 significantly affects the chart’s out-of-control performance. For instance, when $\tau = 0.25$, for every case, the minimum ARL_1 is reached when $p_0 = 0.7$. On the other hand, when $\tau = 2$, the minimum ARL_1 is reached when $p_0 = 0.1$. As a consequence, different initial values for p_0 lead to different results. It is clear that, depending on the shift magnitude to be detected, the initial value of p_0 affects the chart’s out-of-control performance.

Ideally, when *a priori* information for the sample’s underlying distribution is known, practitioners are able to optimize the vector (λ, K, p_0) for a given shift magnitude τ . Nevertheless, this is a strict assumption and it is rarely hold in practice. Moreover, let us keep in mind that the primary motivation of using a nonparametric control chart is the fact that any knowledge of the sample’s distribution is not needed. Consequently, in order to provide a practical implementation and general guidelines to practitioners regarding the “optimal” value of p_0 an extensive numerical analysis will be performed for different distributions. In particular, the out-of-control performance of the proposed chart will be examined under the benchmark of the 18 Johnson’s type distributions listed in Table 1, for different sample sizes and shifts in the process variability. As already stated, we want to investigate, for a variety of distributions, the impact of p_0 to the chart’s optimal out-of-control performance. All the computations regarding the in-control and the out-of-control performance of the chart as well as the determination of the charts’ design parameters were made

via the Markov chain method of Brook and Evans [22], in combination with the "continusify" method of Wu et al. [23] as presented in section 5. The knowledge of the underlying distribution for the out-of-control case is needed only for computing the probability p_1 (see equation (6)) which is associated with the shift magnitude τ . The motivation for this analysis is to examine, for different type of distributions (symmetric/asymmetric), how the optimal value of p_0 varies and to provide guidelines to practitioners about how to select the value of this parameter. This is something that has not been investigated so far in the literature. All the computations have been performed in R [37], on a computer with an Intel(R) Core(TM) i7-7500U CPU. No additional packages have been used except those in the base R edition. The source code is available to the reader upon request. Finally, regarding the optimization procedure, for each distribution, the following steps based on a simple but efficient grid search method have been followed.

- **Step 1:** First we have to define the domain of where the design parameters p_0 and λ will be defined during the searching algorithm. In general, for EWMA schemes, large (small) values of λ are preferable for detecting large (small) shifts in the process variability. So it is logical to define $\lambda \in \{0.05, 0.1, \dots, 0.95\}$. As for the candidate values of p_0 of course we may argue with the fact that p_0 could take any value in the interval $(0, 1)$. However, without loss of generality, it can be simplified by letting p_0 take only a discrete set of values; say $p_0 \in \{0.05, 0.15, \dots, 0.95\}$. This discretisation (which can be regarded as a 'grid search') is justified by the fact that, in practice, only easy-to-manage values of p_0 are meant to be used (for instance, $p_0 = 0.5$ in the original definition of the sign statistic, as already remarked).
- **Step 2:** For each combination of p_0 and λ , we have to properly define the value of K in order to satisfy a desired in-control ARL equal to $ARL_0 = 370.4$. In particular, for every combination of $p_0 \in \{0.05, 0.15, \dots, 0.95\}$ and $\lambda \in \{0.05, 0.1, \dots, 0.95\}$, using the "continusify" method of Wu et al. [23] as presented in section 5 we compute the corresponding value for K under the condition that $ARL_0 = 370.4$ by setting the number of sub-intervals to be equal to $2m + 1 = 151$. Note that, the number $2m + 1 = 151$ has been chosen in order to not be too large but large enough to guarantee the stability of the results. Of course, practitioners can also set any value for $2m + 1 > 151$.
- **Step 3:** Lastly, we should find the optimal values of p_0, λ, K , which minimise the out-of-control ARL for a given shift magnitude. In particular, for each shift $\tau \in \{0.25, 0.5, 0.75, 0.95, 1.25, 1.5, 1.75, 1.95, 2\}$, among all the combinations of (p_0, λ, K) computed in **Step 2**, the optimal vector of (p_0^*, λ^*, K^*) is chosen which gives the smallest out-of-control ARL at a specific shift τ .

In Tables 7 and 8 the optimal combinations of (λ^*, K^*) (first line of each block) are presented, along with the corresponding out-of-control ARL values (second line) and the corresponding pairs of (p_0^*, p_1) (third line) for $n = 10$ (Table 7) and $n = 20$ (Table 8). It should be clarified that p_0^* defines the suggested quantiles for the test for dispersion (i.e., the test statistic SD_t) for a specific value of τ . Also, it is related to the in-control case (i.e. when $p = p_0^*$ we are referring to an in-control process while when, $p \neq p_0^*$ the process is out-of-control). Our conclusions are the following:

- For large decreases in the process variability (e.g., $\tau = 0.25$), it can be seen that, for $p_0^* > 0.6$, the corresponding out-of-control ARL values are $ARL_1 \approx 1$. On the other hand, for large increases ($\tau = 2$), small values for p_0^* are preferable. For

instance, from Table 7 it can be seen that, when $\tau = 0.25$, the optimal value of p_0 is $p_0^* \geq 0.7$. On the other hand, $p_0^* = 0.1$ for large increases (i.e. $\tau = 2$).

- For moderate decreases in the variability (such as $\tau = 0.5$ or 0.75), from Table 7 we may see that p_0^* takes values between 0.3 and 0.6. On the other hand, for moderate increases in the variability ($\tau = 1.5$ or 1.75), the optimal value of p_0 is $p_0^* \leq 0.2$ for all the cases.
- Finally, for small decreases (such as $\tau = 0.95$) or increases ($\tau = 1.25$) the optimal value of p_0 ranges from 0.05 to 0.25.
- Similarly, from Table 8 we may see that all the above statements are also valid for $n = 20$.

From the results presented above, it can be concluded that as the value of τ increases then the optimal value for p_0 decreases. As a general guideline to practitioners, we advise to use $p_0 \approx 0.2$ for a monitoring scheme that aims at the quick detection of small increases/decreases. For moderate shifts, we suggest $p_0 \approx 0.6$. Finally, setting $p_0 \approx 0.1$ and $p_0 \approx 0.7$ can be considered as a reasonable choice for detecting large decreases and increases respectively in the process variability.

6.1. Performance comparisons

In Table 9 the out-of-control performance of the D-SN-C EWMA chart is compared with three parametric Shewhart-type control charts for monitoring the process variability for $n \in \{5, 20, 30\}$ under the normal distribution. In particular, the D-SN-C EWMA chart is compared with the modified R and S charts proposed by Zhang in [36] and an enhanced R chart proposed by Khoo and Lim in [35]. For each case, the proposed chart is optimized as explained in Section 6 assuming a normal distribution. It can be clearly seen that, regardless the sample size or the shift magnitude τ , the D-SN-C EWMA chart has the best performance among its competitors. It should be noted that, for small to moderate decreases ($0.5 < \tau < 0.9$) or increases ($1.1 < \tau < 1.5$), the proposed chart's corresponding ARL_1 values, are significantly smaller, compared with its parametric counterparts. For instance, for $n = 20$, and $\tau = 0.9$ the ARL_1 values for the Zhang's R and S charts and Khoo and Lim's R chart are 188.04, 174.67 and 232.12, respectively, while for the proposed chart it is $ARL_1 = 26.21$. Similarly, when $\tau = 1.1$ the ARL_1 values for the Zhang's R and S chart and Khoo and Lim's R chart are 127.59, 78.82 and 139.9, respectively, while for the proposed chart it is $ARL_1 = 24.47$. As a result, the D-SN-C EWMA chart, can be considered as an efficient choice for monitoring small shifts in the process variance.

Additionally, we compared the performance of the proposed chart with the non-parametric Shewhart-type chart based on the interquantile sign statistic (to be denoted as Shewhart S-SD chart) as introduced by Pawar et al. in [29], under different cases of the Johnson-type distributions introduced above. For both schemes (Shewhart and EWMA), for a given member from the family of Johnson's distributions, we optimised each chart in terms of the value p_0 and computed the quantity

$$\frac{ARL_1^{EWMA} - ARL_1^{Sh}}{ARL_1^{Sh}} \times 100\% \quad (13)$$

where ARL_1^{Sh} (resp. ARL_1^{EWMA}) is the out-of-control performance, in terms of ARL , of the Shewhart S-SD (resp. D-SN-C EWMA) chart, at a given shift in process

variability. These differences are presented in Table 10 for $n = 20$. From the results in Table 10 we deduce that the proposed EWMA chart outperforms the Shewhart S-SD chart, regardless the sample size, the shift magnitude or the underlying distribution.. Practically speaking, for large increases ($\tau > 2$) or decreases ($\tau \rightarrow 0$) in the process variability, these two schemes have similar performance but for small shifts the D-SN-C chart is clearly superior.

Furthermore, except for comparisons with the Shewhart chart of Pawar et al. in [29], we provide next, comparisons with another competitive nonparametric EWMA chart for monitoring the process variability, Specifically, we compare the proposed EWMA chart with the EWMA chart of Yang and Arnold in [17], which is based on the arcsin transformation. We will refer to this chart as the AC-EWMA chart. The out-of-control performance of the AC-EWMA chart is derived by using the same setup as the authors did in [17] (see, Table 9 in [17], page, 2758) assuming Standard Normal and Double Exponential distributions. For the design parameters of the proposed D-SN-C EWMA chart, we set $\lambda = 0.2, K = 2.855$ and $p_0 = 0.2$. We have to note that the choice of $p_0 = 0.2$ is based on the results presented in Section 6. In particular, we showed that, for a symmetric underlying distribution, setting $p_0 \approx 0.2$ significantly improves the ability of the chart to detect small to moderate shifts in the process dispersion. From Table 11, we may see that the proposed chart has better performance regardless the shift magnitude and, therefore, it should be considered as an effective scheme to detect shifts in the process variability.

7. An illustrative example

In this section, an example with two different scenarios is presented, in order to show a practical Phase II implementation of the operation of the proposed D-SN-C EWMA chart. The datasets for each scenario, which have been originally introduced in [38], are presented in Table A1 and plotted in Figures 2 and 3, respectively. Both datasets consists of 30 subgroups of size $n = 5$ where the first 20 subgroups are the same for both scenarios and are randomly generated from the $N(20, 0.1)$ distribution. Moreover, the last 10 subgroups in Figure 2 are generated from the $N(20, 0.2)$ distribution while the last 10 subgroups in Figure 3 are generated from the $N(20, 0.05)$ distribution.

Let us consider a realistic situation, from the point of view of a practitioner, in which we do not have any a priori information regarding the underlying distribution nor the in-control values of the mean and variance for both cases. We only have at our disposal a reference in-control sample of size $n = 30$ and we are interested in monitoring increases (first scenario) and decreases (second scenario) in the process variability. Before we proceed to the phase II implementation of the control chart our primary goal is to:

- determine the value of p_0 as well as the value of the pair (λ, K)
- estimate the quantiles $X_{p_0/2}$ and $X_{1-p_0/2}$.

From the histogram presented in Figure 1 we may see that the in-control reference sample is bell-shaped. Additionally, from the numerical analysis presented in Section 6, we conclude that, for symmetric distributions (or equivalently for cases with light

asymmetry), setting $p_0 \approx 0.05$ and $\lambda \in [0.2, 0.5]$ can be considered as a reasonable choice for detecting moderate increases in the process variability. Similarly for monitoring a moderate decrease in the process variability setting $p_0 \approx 0.45$ and $\lambda \approx 0.2$ can be considered as a reasonable choice. As a consequence, for the current scenarios, the vector of parameters (p_0^*, λ^*, K^*) for detecting an increase in the process dispersion is chosen to be $(p_0^* = 0.05, \lambda^* = 0.25, K^* = 3.424)$ with the corresponding control limits $LCL^* = -5.789$, $UCL^* = -3.212$ computed using (11) and (12) presented in Section 5 where the value of the “continuousify” parameter is set to $h = 0.2$. Similarly, for detecting a decrease in the process dispersion we choose the vector $(p_0^* = 0.5, \lambda^* = 0.25, K^* = 2.823)$ and the control limits are equal to $LCL^* = -2.395$, $UCL^* = 2.395$.

Regarding the determination of the quantiles of interest for each scenario the simplest way is to estimate them from the reference sample through the inverse of its empirical distribution. In particular, for $p_0 = 0.5$ the estimates of the $X_{p_0/2}$ and $X_{1-p_0/2}$ are equal to $\hat{X}_{0.25} = 19.96594$ (the theoretical values assuming normality is 19.8651) and $\hat{X}_{0.75} = 20.0928$ (the theoretical value assuming normality is 20.1349). Similarly, for $p_0 = 0.05$ the estimates of the $X_{p_0/2}$ and $X_{1-p_0/2}$ are equal to $\hat{X}_{0.025} = 19.8436$ and $\hat{X}_{0.975} = 20.2296$. (the theoretical values assuming normality are 19.60801 and 20.39199).

Finally, the corresponding values of SD_t , SD_t^* and Z_t^* are presented in Table 12. From Figure 4, it can be seen that the proposed chart can efficiently detect the increase in the process variability at the 25th sampling point. Similarly, for the second scenario, which corresponds to a decrease in the process variability (Figure 5), we may see that the D-SN-C EWMA chart also detects this shift at the 25th sampling point.

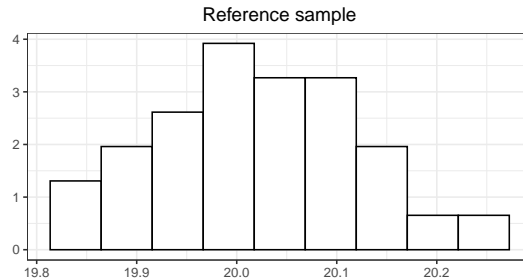


Figure 1.: Histogram of the reference sample

8. Conclusions

In this paper, we introduced a nonparametric EWMA control chart based on a general extension of the Sign statistic, called as the D-SN-C EWMA chart, for monitoring shifts in the process variability. For the computation of the chart’s RL properties, the “continuousify” method of Wu et al. [23] has been used, ensuring that the ARL values can be accurately and effectively calculated. Additionally, the

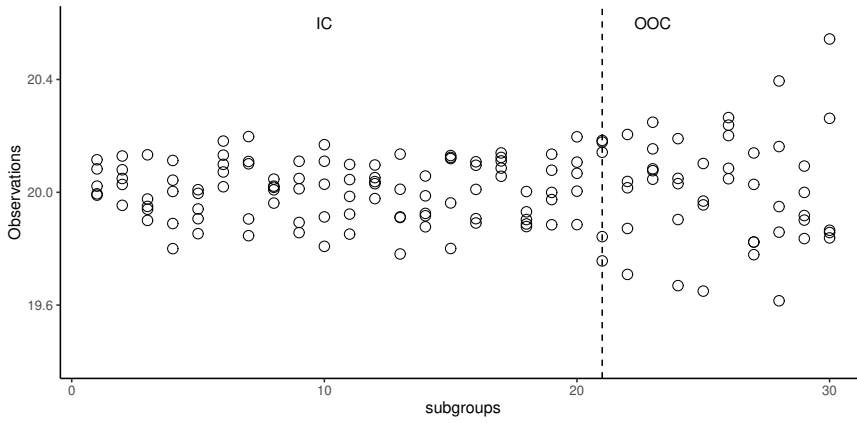


Figure 2.: Dataset for the first example

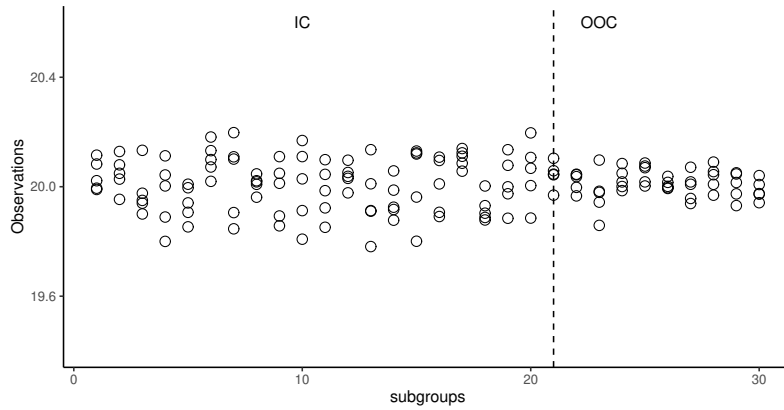


Figure 3.: Dataset for the second example

chart’s out-of-control performance has been examined under a benchmark of 18 Johnson’s type distributions covering a wide range of symmetric and asymmetric distributions. Based on our results, when the value of the in-control parameter p_0 is optimized (instead of being pre-defined), the chart’s out-of-control performance is significantly improved; more precisely, values of $p_0 \approx 0.2$ are found to be preferable for small decreases ($\tau \approx 0.95$) or increases ($\tau \approx 1.25$). Additionally, for large decreases ($\tau \approx 0.25$) or increases ($\tau \approx 2$) in the process variability, large ($p_0 \approx 0.7$) or small values ($p_0 \approx 0.05$) of p_0 are respectively the optimal ones. As a consequence, the proposed chart can be considered as a reliable technique which provides to the practitioners robust information regarding its in- and out-of-control RL properties.

The current work can be extended in several directions. In particular, the “continuousify” method could be applied in EWMA schemes where other nonparametric statistics are considered such as the Mann-Whitney, or the Ansari-Bradley statistics. Additionally, it would also be interesting to examine the performance of the proposed EWMA chart based on the general Sign statistic under the presence of ties in the pop-

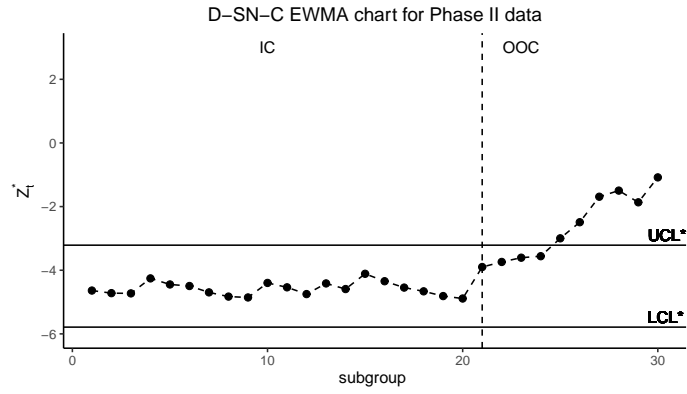


Figure 4.: The D-SN-C EWMA chart for the Phase II data presented in Figure 2

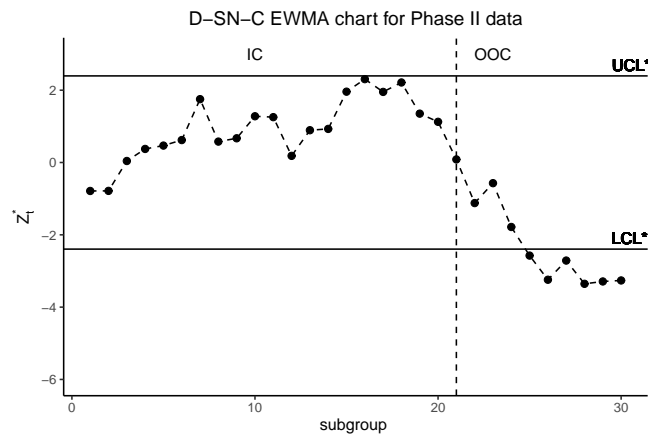


Figure 5.: The D-SN-C EWMA chart for the Phase II data presented in Figure 3

ulation. Finally, the method of Wu et al. [23] could be extended in distribution-free EWMA charts designed for monitoring bivariate processes.

Acknowledgements

The authors would like to express their gratitude to the Editor and the two anonymous reviewers for their constructive comments which improved the content and the presentation of this paper.

VGB's research work was supported by the Ministerio de Ciencia e Innovación of Spain under grant no. PID2019-110442GB-I00.

Appendix

Let $E_N(X) = \mu$ and $V_N(X) = h^2$ denote the mean and variance of a random variable, X , from a Normal distribution. Then the mean of SD_t^* , is computed as:

$$\begin{aligned}
E(SD_t^*) &= \int_{-\infty}^{\infty} s \times f_{SD_t^*}(s|n, p_1) ds \\
&= \int_{-\infty}^{\infty} s \times \sum_{\psi \in \Psi} f_{\text{Bin}}\left(\frac{\psi+n}{2}|n, p_1\right) \times f_N(s|\psi, h) ds \\
&= \sum_{\psi \in \Psi} \left[f_{\text{Bin}}\left(\frac{\psi+n}{2}|n, p_1\right) \times \int_{-\infty}^{\infty} s \times f_N(s|\psi, h) ds \right] \\
&= \sum_{\psi \in \Psi} \left[f_{\text{Bin}}\left(\frac{\psi+n}{2}|n, p_1\right) \times E_N(s) \right] \\
&= \sum_{\psi \in \Psi} \left[f_{\text{Bin}}\left(\frac{\psi+n}{2}|n, p_1\right) \times \psi \right] \\
&= E(SD_t)
\end{aligned}$$

Similarly, using the fact that $E(SD_t^*) = E(SD_t)$ the variance of SD_t^* is computed as:

$$\begin{aligned}
V(SD_t^*) &= E(SD_t^*)^2 - (E(SD_t^*))^2 \\
&= \int_{-\infty}^{\infty} s^2 \times f_{SD_t^*}(s|n, p_1) ds - (E(SD_t^*))^2 \\
&= \int_{-\infty}^{\infty} s^2 \times \sum_{\psi \in \Psi} \left[f_{\text{SD}}\left(\frac{\psi+n}{2}|n, p_1\right) \times f_N(s|\psi, h) \right] ds - (E(SD_t))^2 \\
&= \sum_{\psi \in \Psi} \left[f_{\text{Bin}}\left(\frac{\psi+n}{2}|n, p_1\right) \times \int_{-\infty}^{\infty} s^2 \times f_N(s|\psi, h) ds \right] - (E(SD_t))^2 \\
&= \sum_{\psi \in \Psi} \left[f_{\text{Bin}}\left(\frac{\psi+n}{2}|n, p_1\right) \times E_N(s^2) \right] - (E(SD_t))^2 \\
&= \sum_{\psi \in \Psi} \left[f_{\text{Bin}}\left(\frac{\psi+n}{2}|n, p_1\right) \times (V_N(s) + (E_N(s))^2) \right] - (E(SD_t))^2 \\
&= \sum_{\psi \in \Psi} \left[f_{\text{Bin}}\left(\frac{\psi+n}{2}|n, p_1\right) \times (h^2 + \psi^2) \right] - (E(SD_t))^2 \\
&= h^2 \times \sum_{\psi \in \Psi} f_{\text{Bin}}\left(\frac{\psi+n}{2}|n, p_1\right) + \sum_{\psi \in \Psi} \psi^2 \times f_{\text{Bin}}\left(\frac{\psi+n}{2}|n, p_1\right) - (E(SD_t))^2 \\
&= h^2 + E(SD_t)^2 - (E(SD_t))^2 \\
&= h^2 + V(SD_t).
\end{aligned}$$

Table A1.: Phase II samples of $t = 1, 2, \dots, 20$ subgroups of size $n = 5$

		Subgroup																			
		1	2	3	4	5	6	7	8	9	10	11	12	13	14	15	16	17	18	19	20
First 20 subgroups for both examples																					
$X_{t,j}$	1	20.083	20.028	19.950	19.889	19.941	20.020	20.101	20.022	20.049	20.169	20.099	19.978	20.135	19.878	20.130	20.010	20.086	19.888	20.000	19.885
	2	20.115	20.129	19.900	20.043	19.996	20.072	20.109	20.009	20.013	19.808	19.923	20.052	20.011	19.917	20.120	20.096	20.124	19.931	19.974	20.107
	3	19.990	19.954	19.940	20.003	20.009	20.182	19.846	20.018	20.110	20.110	20.045	20.038	19.911	19.925	20.124	19.906	20.140	19.903	20.078	20.004
	4	20.022	20.080	20.133	19.800	19.853	20.132	20.198	20.047	19.893	20.029	19.985	20.097	19.913	19.988	19.801	20.108	20.057	20.003	20.135	20.067
	5	19.995	20.049	19.976	20.113	19.906	20.099	19.905	19.962	19.857	19.913	19.852	20.031	19.781	20.058	19.962	19.891	20.111	19.878	19.885	20.197
Last 10 subgroups for example 1 (Figure 2)																					
$X_{t,j}$	21	22	23	24	25	26	27	28	29	30											
	1	19.843	20.038	20.077	20.031	19.650	20.265	20.028	20.162	20.000	20.544										
	2	20.142	19.709	20.046	20.190	19.396	20.085	20.139	19.949	20.093	19.865										
	3	19.757	19.872	20.154	19.903	19.969	20.201	19.824	19.859	19.901	19.857										
	4	20.184	20.016	20.083	19.669	19.955	20.238	19.779	20.395	19.836	20.262										
	5	20.178	20.205	20.248	20.049	20.102	20.048	19.824	19.615	19.918	19.838										
Last 10 subgroups for example 2 (Figure 3)																					
$X_{t,j}$	21	22	23	24	25	26	27	28	29	30											
	1	20.044	20.044	20.097	20.049	20.018	19.994	19.957	20.044	20.047	19.942										
	2	20.046	20.037	19.859	20.001	20.003	20.038	20.009	19.969	20.051	19.975										
	3	20.058	19.966	19.983	20.085	20.076	20.001	20.018	20.009	19.931	20.041										
	4	20.104	20.046	19.944	19.986	20.087	20.016	20.071	20.090	19.974	20.008										
	5	19.969	19.998	19.979	20.018	20.070	19.996	19.939	20.055	20.015	19.973										

References

- [1] Shewhart, W.A. (1926). Quality Control Charts, *The Bell System Technical Journal*, 5(4), 593–603.
- [2] Page, E.S. (1954), Continuous Inspection Schemes, *Biometrika*, 41(1/2), 100–115.
- [3] Roberts, SW. (1959). Control Chart Tests Based on Geometric Moving Averages, *Technometrics*, 1, 239–250.
- [4] Amin, R.W., Searcy, A.J. (1991). A Nonparametric Exponentially Weighted Moving Average Control Scheme, *Communications in Statistics-Simulation and Computation*, 20(4), 1049–1072.
- [5] Graham, M.A., Chakraborti, S., Human, S.W. (2011). A Nonparametric EWMA Sign Chart for Location Based on Individual Measurements, *Quality Engineering*, 23(3), 227–241
- [6] Yang, S.-F., Lin, J.-S., Cheng, S.W. (2011). A New Nonparametric EWMA Sign Control Chart, *Expert Systems with Applications*, 38(5), 6239–6243.
- [7] Aslam, M., Azam, M., Jun, C.H. (2014). A New Exponentially Weighted Moving Average Sign Chart using Repetitive Sampling, *Journal of Process Control*, 24(7), 1149–1153.
- [8] Riaz, M. (2015). A Sensitive Non-Parametric EWMA Control Chart, *Journal of the Chinese Institute of Engineers*, 38(2), 208–219.
- [9] Lu, S.L. (2015). An Extended Nonparametric Exponentially Weighted Moving Average Sign Control Chart, *Quality and Reliability Engineering International*, 31(1), 3–13.
- [10] Haq, A. (2019). A New Nonparametric Synthetic EWMA Control Chart for Monitoring Process Mean, *Communications in Statistics-Simulation and Computation*, 48(6), 1665–1676.
- [11] Amin, R.W., Reynolds, Jr.MR., Bakir, S. (1995). Nonparametric Quality control Charts based on the Sign Statistic, *Communications in Statistics-Theory and Methods*, 24(6), 1597–1623.
- [12] Murakami, H., Matsuki, T. (2010). A Nonparametric Control Chart Based on the Mood Statistic for Dispersion, *The International Journal of Advanced Manufacturing Technology*, 49(5-8), 757–763.
- [13] Das, N., Bhattacharya, A. (2008). A New Non-Parametric Control Chart for Controlling Variability, *Quality Technology & Quantitative Management*, 5(4), 351–361.
- [14] Das, N. (2008). A Note on the Efficiency of Nonparametric Ccontrol Chart for Monitoring Process Variability, *Economic Quality Control*, 23(1), 85–93.
- [15] Zou, C., Tsung, F. (2010). Likelihood Ratio-Based Distribution-free EWMA Control Charts, *Journal of Quality Technology*, 42(2), 174–196.
- [16] Chowdhury, S., Mukherjee, A., Chakraborti, S. (2015). Distribution-free Phase II CUSUM Control Chart for Joint Monitoring of Location and Scale, *Quality and Reliability Engineering International*, 31(1), 135–151.
- [17] Yang, S-F., Arnold, B-C. (2016). A New Approach for Monitoring Process Variance, *Journal of Statistical Computation and Simulation*, 86(14), 2749–2765.
- [18] Haq, A. (2017). A New Nonparametric EWMA Control Chart for Monitoring Process Variability, *Quality and Reliability Engineering International*, 33(7), 1499–1512.
- [19] Mukherjee, A., Marozzi, M. (2017). A Distribution-free Phase-II CUSUM Procedure for Monitoring Service Quality, *Total Quality Management & Business Excellence*, 28(11-12), 1227–1263.
- [20] Chakraborti, S., Van der Laan, P., Bakir, S.T. (2001). Nonparametric Control Charts: an Overview and Some Results, *Journal of Quality Technology*, 33(3), 304–315.
- [21] Chakraborti, S., Graham, M.A. (2019). Nonparametric (Distribution-Free) Control Charts: An Updated Overview and Some Result, *Quality Engineering*, 31(4), 523–544.
- [22] Brook, D., Evans, D.A. (1972). An Approach to the Probability Distribution of CUSUM Run Length, *Biometrika*, 59(3), 539–549.
- [23] Wu, S, Castagliola, P, Celano, G. (2020). A Distribution-free EWMA Control Chart for Monitoring Time-Between-Events-and-Amplitude Data, *Journal of Applied Statistics*,

- 3(48), 434–454.
- [24] Perdikis, T., Psarakis, S., Castagliola, P., Maravelakis, P.E. (2021). An EWMA Signed Ranks Control Chart with Reliable Run Length Performances, *Quality and Reliability Engineering International*, 37(3), 1266-1284.
- [25] Castagliola, P., Tran, K.P., Celano, G., Rakitzis, A.C., Maravelakis, P.E. (2019). An EWMA-Type Sign Chart With Exact Run Length Properties, *Journal of Quality Technology*, 51(1), 51–63.
- [26] Rakitzis, A.C., Castagliola, P., Maravelakis, P.E. (2015). A New Memory-type Monitoring Technique for Count Data, *Computers & Industrial Engineering*, 85, 235–247.
- [27] Tang, A., Sun, J., Hu, X., Castagliola, P. (2019). A New Nonparametric Adaptive EWMA Control Chart with Exact Run Length Properties, *Computers & Industrial Engineering*, 130, 404–419.
- [28] Perdikis, T. Psarakis, S. Castagliola, P. Celano, G. (2021). An EWMA-type Chart based on Signed Ranks with Exact Run Length Properties, *Journal of Statistical Computation and Simulation*, 91(4), 732-751.
- [29] Pawar, V.Y, Shirke, D.T, Khilare,S.K (2018) A Nonparametric Control Chart for Process Variability Based on Quantiles, *International Journal of Statistics and Economics*, 19(3), 55–64.
- [30] Neuts, M.F. (1981).Matrix-Geometric Solutions in Stochastic Models: An Algorithmic Approach,*Dover Publications Inc,New York*.
- [31] Latouche, G., Ramaswami V. (1999). Introduction to Matrix Analytic Methods in Stochastic Modeling,*ASA-SIAM,Philadelphia*.
- [32] Castagliola P., Tran, K.P., Celano, G., Maravelakis, P.E. (2020). The Shewhart Sign Chart with Ties: Performance and Alternatives, *Distribution-Free Methods for Statistical Process Monitoring and Control*, 107–136, Springer
- [33] Wu, S., Castagliola, P.,Rakitzis, A.C., Maravelakis, P.E. (2021). Design of Attribute EWMA Type Control Charts with Reliable Run Length Performance, *Communications in Statistics - Simulation and Computation*, doi = 10.1080/03610918.2021.1955263
- [34] Perdikis, T., Psarakis, S., Castagliola, P.,Rakitzis, A.C., Maravelakis P.E. (2021). The EWMA Sign Chart Revisited: Performance and Alternatives Without and With Ties, *Journal of Applied Statistics*, doi = 10.1080/02664763.2021.1982879
- [35] Khoo, M-B.C, Lim, E.G. (2005) An Improved R (range) Control Chart for Monitoring the Process Variance, *Quality and Reliability Engineering International*, 21(1), 43–50.
- [36] Yhang, G. (2014) Improved R and S Control Charts for Monitoring the Process Variance, *Journal of Applied Statistics*, 41(6), 1260–1273.
- [37] R Core Team,(2021).R: A Language and Environment for Statistical Computing, R Foundation for Statistical Computing,Vienna, Austria.
- [38] Castagliola, P., Celano, G., Fichera, S. (2006). Monitoring Process Variability using EWMA, *Handbook of Engineering Statistics*, 291–325, Springer.

Table 2.: In-control values of ARL for the D-SN EWMA and D-SN-C EWMA charts when $\lambda = 0.2$, $K = 2.85$ and $h = 0.2$ under different combinations of (n, p_0) .

$2m+1$	$(n = 12, p_0 = 0.3)$		$(n = 12, p_0 = 0.5)$		$(n = 12, p_0 = 0.9)$		$(n = 12, p_0 = 0.8)$	
	D-SN EWMA	D-SN-C EWMA	D-SN EWMA	D-SN-C EWMA	D-SN EWMA	D-SN-C EWMA	D-SN EWMA	D-SN-C EWMA
51	364.3	379.6	418.1	382.6	371.9	380.3	386.6	363.7
61	349.6	380.6	372.9	382.6	361.8	381.4	378.2	364.3
71	394.1	381.1	382.9	383.1	380.6	381.9	368.0	364.7
81	381.3	381.4	399.6	383.4	389.2	382.2	366.7	364.9
91	385.5	381.6	397.7	383.6	399.1	382.5	371.0	365.1
101	386.0	381.7	386.6	383.8	385.6	382.6	371.1	365.3
111	385.7	381.8	389.5	383.9	380.1	382.7	365.7	365.3
121	382.3	381.9	388.3	384.0	371.8	382.8	368.8	365.4
131	378.1	381.9	391.8	384.1	388.1	382.9	365.1	365.5
141	386.0	382.0	372.5	384.1	391.8	382.9	358.9	365.5
151	382.9	382.0	375.5	384.2	381.2	383.0	366.8	365.6
161	380.7	382.0	375.8	384.2	382.7	383.0	359.2	365.6
171	381.5	382.1	372.7	384.2	383.1	383.1	361.6	365.6
181	395.5	382.1	382.2	384.3	386.8	383.1	367.7	365.6
191	383.5	382.1	382.6	384.3	378.1	383.1	362.8	365.7
201	377.6	382.1	386.1	384.3	381.5	383.1	358.2	365.7
sim	(382)		(383.1)		(382.5)		(364.5)	

$2m+1$	$(n = 20, p_0 = 0.3)$		$(n = 20, p_0 = 0.5)$		$(n = 20, p_0 = 0.6)$		$(n = 20, p_0 = 0.8)$	
	D-SN EWMA	D-SN-C EWMA	D-SN EWMA	D-SN-C EWMA	D-SN EWMA	D-SN-C EWMA	D-SN EWMA	D-SN-C EWMA
51	392.2	371.7	347.4	370.7	358.9	372.4	359.7	360.7
61	386.9	373.2	381.8	375.4	385.1	375.3	365.1	361.7
71	385.7	372.7	372.0	375.4	389.0	375.5	348.1	361.7
81	378.1	372.9	384.4	375.9	397.3	375.8	349.6	361.9
91	378.9	373.1	376.9	376.1	383.8	375.9	360.4	362.4
101	372.3	373.2	382.1	376.2	357.1	375.9	360.0	362.5
111	358.0	373.3	377.8	376.3	379.3	376.0	361.1	362.6
121	382.8	373.3	389.0	376.4	380.6	376.1	360.5	362.7
131	372.5	373.4	375.3	376.5	380.6	376.2	355.9	362.8
141	365.9	373.4	372.5	376.5	374.1	376.2	371.3	362.8
151	369.7	373.4	368.5	376.5	382.9	376.2	364.2	362.9
161	371.5	373.5	375.2	376.6	372.5	376.3	369.4	362.9
171	361.3	373.5	376.8	376.6	380.5	376.3	362.8	362.9
181	378.1	373.5	376.6	376.6	377.1	376.3	361.7	363.0
191	377.2	373.5	375.1	376.6	374.5	376.3	370.7	363.0
201	377.1	373.5	377.3	376.7	378.5	376.3	368.5	363.0
sim	(372.7)		(375.6)		(376.2)		(360.06)	

Table 3.: ARL_1 values as a function of the number of subintervals $2m + 1$ for the two-sided D-SN EWMA chart (top) and two-sided D-SN-C EWMA chart (bottom) with $h = 0.2$ when $\lambda = 0.2$, $K = 2.85$, $n = 5$ and $\tau = 1.1$ for the #1–#18 distributions listed in Table 1.

D-SN EWMA chart																		
$2m + 1$	#1	#2	#3	#4	#5	#6	#7	#8	#9	#10	#11	#12	#13	#14	#15	#16	#17	#18
51	158.6	182.1	188.8	193.7	198.7	202.8	164.6	180.9	185.4	194.8	202.3	207.3	168.5	176.9	179.2	200.8	211.4	217.2
61	178.9	206.4	214.3	220.1	226.1	230.9	185.9	205.0	210.4	221.4	230.3	236.3	190.5	200.3	203.0	228.6	241.1	248.1
71	162.6	187.1	194.2	199.3	204.6	208.8	168.8	185.8	190.6	200.4	208.3	213.6	173.0	181.7	184.1	206.8	217.9	224.0
81	170.9	196.8	204.3	209.7	215.3	219.7	177.5	195.5	200.6	210.9	219.3	224.8	181.9	191.1	193.6	217.6	229.4	235.8
91	174.9	201.8	209.6	215.2	221.1	225.8	181.7	200.5	205.7	216.5	225.3	231.1	186.3	195.9	198.5	223.5	235.9	242.7
101	176.3	203.3	211.1	216.8	222.7	227.3	183.2	201.9	207.2	218.0	226.8	232.7	187.7	197.3	200.0	225.1	237.4	244.2
111	172.0	198.3	205.9	211.4	217.1	221.6	178.7	197.0	202.1	212.6	221.1	226.8	183.1	192.5	195.0	219.4	231.4	238.0
121	179.5	207.3	215.3	221.1	227.2	232.0	186.6	205.9	211.3	222.4	231.5	237.5	191.2	201.1	203.8	229.7	242.4	249.4
131	167.2	192.6	199.9	205.2	210.7	215.1	173.7	191.3	196.3	206.4	214.6	220.1	177.9	187.0	189.4	213.0	224.5	230.9
141	169.9	195.7	203.1	208.5	214.1	218.5	176.5	194.4	199.4	209.7	218.0	223.6	180.8	190.0	192.5	216.4	228.1	234.6
151	163.9	188.6	195.7	200.8	206.2	210.4	170.2	187.3	192.2	202.0	210.0	215.3	174.4	183.1	185.5	208.4	219.6	225.8
161	174.7	201.4	209.2	214.7	220.6	225.2	181.5	200.1	205.3	216.0	224.7	230.5	186.0	195.5	198.1	222.9	235.1	241.8
171	170.4	196.3	203.8	209.2	214.9	219.4	177.0	195.0	200.1	210.5	218.9	224.5	181.4	190.6	193.1	217.2	229.0	235.5
181	169.1	194.8	202.2	207.5	213.1	217.5	175.6	193.4	198.5	208.7	217.0	222.6	179.9	189.1	191.6	215.4	227.1	233.5
191	173.2	199.6	207.3	212.8	218.6	223.2	179.9	198.3	203.5	214.1	222.7	228.4	184.4	193.8	196.4	221.0	233.1	239.7
201	172.2	198.4	206.0	211.4	217.1	221.7	178.9	197.1	202.2	212.7	221.2	226.8	183.3	192.6	195.2	219.5	231.4	238.0
stm	170.0	198.0	202.5	209.5	216.1	218.9	175.9	194.8	200.9	212.2	220.0	226.0	181.9	192.0	193.8	218.5	230.3	237.0

D-SN-C EWMA chart																		
$2m + 1$	#1	#2	#3	#4	#5	#6	#7	#8	#9	#10	#11	#12	#13	#14	#15	#16	#17	#18
51	171.0	196.8	204.3	209.6	215.2	219.7	177.6	195.5	200.6	210.8	219.2	224.8	181.9	191.1	193.6	217.5	229.3	235.7
61	171.2	197.1	204.6	210.0	215.6	220.1	177.8	195.8	200.9	211.2	219.6	225.2	182.2	191.4	193.9	217.9	229.7	236.2
71	171.4	197.3	204.8	210.2	215.8	220.3	178.0	196.0	201.1	211.4	219.8	225.4	182.3	191.6	194.1	218.1	229.9	236.4
81	171.5	197.4	204.9	210.3	216.0	220.4	178.1	196.1	201.2	211.5	219.9	225.6	182.5	191.7	194.2	218.3	230.1	236.6
91	171.5	197.5	205.0	210.4	216.1	220.5	178.2	196.2	201.3	211.6	220.0	225.7	182.5	191.8	194.3	218.4	230.2	236.7
101	171.6	197.6	205.1	210.5	216.1	220.6	178.2	196.2	201.3	211.7	220.1	225.7	182.6	191.8	194.4	218.4	230.3	236.8
111	171.6	197.6	205.1	210.5	216.2	220.7	178.2	196.3	201.4	211.8	220.2	225.8	182.6	191.9	194.4	218.5	230.3	236.8
121	171.7	197.6	205.1	210.6	216.2	220.7	178.3	196.3	201.4	211.8	220.2	225.8	182.6	191.9	194.4	218.5	230.4	236.9
131	171.7	197.7	205.2	210.6	216.2	220.7	178.3	196.3	201.4	211.8	220.2	225.9	182.7	191.9	194.5	218.6	230.4	236.9
141	171.7	197.7	205.2	210.6	216.3	220.8	178.3	196.4	201.5	211.8	220.3	225.9	182.7	191.9	194.5	218.6	230.4	236.9
151	171.7	197.7	205.2	210.6	216.3	220.8	178.3	196.4	201.5	211.9	220.3	225.9	182.7	192.0	194.5	218.6	230.5	237.0
161	171.7	197.7	205.2	210.6	216.3	220.8	178.3	196.4	201.5	211.9	220.3	225.9	182.7	192.0	194.5	218.6	230.5	237.0
171	171.7	197.7	205.2	210.7	216.3	220.8	178.4	196.4	201.5	211.9	220.3	225.9	182.7	192.0	194.5	218.6	230.5	237.0
181	171.7	197.7	205.3	210.7	216.3	220.8	178.4	196.4	201.5	211.9	220.3	225.9	182.7	192.0	194.5	218.7	230.5	237.0
191	171.7	197.8	205.3	210.7	216.3	220.8	178.4	196.4	201.5	211.9	220.3	226.0	182.7	192.0	194.5	218.7	230.5	237.0
201	171.7	197.8	205.3	210.7	216.3	220.8	178.4	196.4	201.5	211.9	220.3	226.0	182.7	192.0	194.5	218.7	230.5	237.0
p_1	0.5463	0.5411	0.5398	0.5388	0.5378	0.5371	0.5449	0.5414	0.5404	0.5386	0.5371	0.5362	0.5440	0.5422	0.5417	0.5374	0.5355	0.5344

Table 4.: ARL_1 values as a function of the number of subintervals $2m + 1$ for the two-sided D-SN EWMA chart (top) and two-sided D-SN-C EWMA chart (bottom) with $h = 0.2$ when $\lambda = 0.2$, $K = 2.85$, $n = 5$ and $\tau = 0.9$ for the #1–#18 distributions listed in Table 1

D-SN EWMA chart																		
$2m + 1$	#1	#2	#3	#4	#5	#6	#7	#8	#9	#10	#11	#12	#13	#14	#15	#16	#17	#18
51	120.2	149.7	158.3	164.4	170.7	175.7	121.4	146.2	152.9	165.4	175.0	181.3	125.6	139.1	142.7	173.0	186.3	193.3
61	134.2	168.5	178.5	185.7	193.1	198.9	135.6	164.4	172.2	186.8	198.1	205.5	140.5	156.1	160.3	195.7	211.4	219.7
71	122.6	153.4	162.3	168.6	175.2	180.4	124.0	149.7	156.6	169.7	179.7	186.3	128.3	142.3	146.0	177.6	191.5	198.9
81	128.7	161.2	170.6	177.3	184.3	189.8	130.1	157.3	164.6	178.4	189.0	196.0	134.7	149.5	153.5	186.8	201.5	209.3
91	131.2	164.7	174.5	181.5	188.8	194.5	132.6	160.7	168.3	182.7	193.7	200.9	137.3	152.6	156.7	191.4	206.7	214.9
101	132.3	166.1	175.9	182.9	190.2	196.0	133.8	162.1	169.7	184.1	195.2	202.4	138.6	153.9	158.1	192.8	208.2	216.4
111	129.3	162.1	171.7	178.5	185.6	191.2	130.7	158.2	165.6	179.6	190.4	197.4	135.3	150.3	154.3	188.1	203.1	211.0
121	134.4	169.0	179.1	186.3	193.8	199.7	135.9	164.9	172.7	187.5	198.9	206.4	140.8	156.5	160.8	196.5	212.3	220.7
131	125.9	157.7	166.9	173.5	180.3	185.7	127.3	153.9	161.0	174.5	185.0	191.7	131.8	146.2	150.1	182.7	197.2	204.8
141	127.9	160.2	169.6	176.3	183.2	188.7	129.3	156.3	163.6	177.4	187.9	194.8	133.9	148.6	152.5	185.7	200.3	208.1
151	123.7	154.6	163.6	170.0	176.7	181.9	125.0	150.9	157.9	171.1	181.2	187.8	129.4	143.5	147.3	179.0	193.1	200.5
161	131.3	164.7	174.3	181.3	188.5	194.2	132.7	160.7	168.2	182.4	193.4	200.6	137.4	152.6	156.7	191.1	206.3	214.4
171	128.2	160.6	170.0	176.8	183.8	189.3	129.6	156.7	164.1	177.9	188.6	195.5	134.2	148.9	152.9	186.3	201.0	208.9
181	127.3	159.4	168.7	175.4	182.3	187.8	128.6	155.6	162.8	176.5	187.0	193.9	133.2	147.8	151.7	184.8	199.4	207.2
191	130.1	163.2	172.8	179.7	186.8	192.5	131.5	159.2	166.7	180.8	191.7	198.8	136.2	151.3	155.3	189.4	204.5	212.5
201	129.6	162.3	171.9	178.7	185.7	191.3	131.0	158.4	165.8	179.8	190.6	197.6	135.6	150.5	154.5	188.2	203.2	211.1
sim	128.7	162.8	172.2	178.0	184.1	190.6	130.6	157.8	166.4	178.0	190.0	197.7	135.8	150.0	154.1	188.1	202.5	212.0

D-SN-C EWMA chart																		
$2m + 1$	#1	#2	#3	#4	#5	#6	#7	#8	#9	#10	#11	#12	#13	#14	#15	#16	#17	#18
51	128.8	161.2	170.6	177.4	184.3	189.8	130.2	157.4	164.7	178.4	189.1	196.0	134.8	149.6	153.5	186.8	201.5	209.3
61	129.0	161.5	170.9	177.6	184.6	190.1	130.4	157.6	164.9	178.7	189.4	196.3	135.0	149.8	153.7	187.1	201.8	209.6
71	129.1	161.6	171.0	177.8	184.8	190.3	130.5	157.7	165.0	179.0	189.5	196.5	135.1	149.9	153.9	187.2	202.0	209.8
81	129.1	161.7	171.1	177.9	184.9	190.4	130.5	157.8	165.1	179.0	189.6	196.6	135.1	150.0	153.9	187.3	202.1	210.0
91	129.2	161.7	171.2	178.0	185.0	190.5	130.6	157.9	165.2	179.0	189.7	196.7	135.2	150.0	154.0	187.4	202.2	210.1
101	129.2	161.8	171.2	178.0	185.0	190.5	130.6	157.9	165.2	179.1	189.8	196.7	135.2	150.1	154.0	187.5	202.3	210.1
111	129.2	161.8	171.3	178.0	185.0	190.6	130.6	158.0	165.3	179.1	189.8	196.8	135.2	150.1	154.1	187.5	202.3	210.2
121	129.3	161.8	171.3	178.1	185.1	190.6	130.7	158.0	165.3	179.2	189.8	196.8	135.3	150.1	154.1	187.5	202.4	210.2
131	129.3	161.9	171.3	178.1	185.1	190.6	130.7	158.0	165.3	179.2	189.9	196.8	135.3	150.1	154.1	187.6	202.4	210.3
141	129.3	161.9	171.3	178.1	185.1	190.6	130.7	158.0	165.3	179.2	189.9	196.9	135.3	150.1	154.1	187.6	202.4	210.3
151	129.3	161.9	171.3	178.1	185.1	190.6	130.7	158.0	165.3	179.2	189.9	196.9	135.3	150.1	154.1	187.6	202.4	210.3
161	129.3	161.9	171.3	178.1	185.1	190.7	130.7	158.0	165.4	179.2	189.9	196.9	135.3	150.2	154.1	187.6	202.4	210.3
171	129.3	161.9	171.4	178.1	185.2	190.7	130.7	158.0	165.4	179.2	189.9	196.9	135.3	150.2	154.1	187.6	202.5	210.3
181	129.3	161.9	171.4	178.1	185.2	190.7	130.7	158.0	165.4	179.2	189.9	196.9	135.3	150.2	154.2	187.6	202.5	210.3
191	129.3	161.9	171.4	178.2	185.2	190.7	130.7	158.0	165.4	179.2	189.9	196.9	135.3	150.2	154.2	187.6	202.5	210.3
201	129.3	161.9	171.4	178.2	185.2	190.7	130.7	158.0	165.4	179.3	190.0	196.9	135.3	150.2	154.2	187.7	202.5	210.3
p_1	0.4431	0.4515	0.4536	0.4550	0.4564	0.4575	0.4435	0.4506	0.4523	0.4553	0.4574	0.4587	0.4448	0.4487	0.4497	0.4569	0.4597	0.4611

Table 5.: ARL_0 values of the two-sided D-SN-C EWMA chart for $\lambda = 0.2$, $K = 2.85$ and for fixed values of $h = \{0.1, 0.15, \dots, 0.3\}$ and different combinations of (n, p_0) .

$2m+1$	$(n, p_0) = (7, 0.4)$				$(n, p_0) = (13, 0.5)$				$(n, p_0) = (15, 0.6)$			
	0.1	0.15	0.2	0.3	0.1	0.15	0.2	0.3	0.1	0.15	0.2	0.3
51	380.2	379.8	379.7	379.7	408.8	404.4	403.4	403.2	376.4	376.8	377.1	377.2
61	380.7	380.6	380.6	380.5	402.5	403.9	404.1	404.1	380.7	378.9	378.2	378.1
71	380.9	381.0	381.0	381.0	402.5	404.6	404.7	404.5	374.3	377.5	378.4	378.5
81	381.0	381.3	381.3	381.2	405.2	405.1	405.1	404.9	378.7	378.7	378.8	378.8
91	381.7	381.6	381.5	381.4	405.6	405.3	405.4	405.1	378.9	378.9	379.0	379.0
101	381.6	381.7	381.7	381.6	405.5	405.5	405.5	405.3	379.9	379.1	379.1	379.2
111	381.8	381.8	381.8	381.6	405.6	405.6	405.7	405.3	379.2	379.2	379.3	379.2
121	381.9	381.9	381.9	381.8	405.7	405.8	405.8	405.6	379.2	379.3	379.4	379.3
131	381.9	382.0	382.0	381.8	405.8	405.8	405.9	405.6	379.2	379.4	379.4	379.4
141	382.0	382.0	382.0	381.9	405.9	405.9	405.9	405.7	379.4	379.4	379.5	379.4
151	382.1	382.1	382.1	382.0	405.9	406.0	406.0	405.9	379.4	379.5	379.5	379.5
161	382.1	382.1	382.1	382.0	406.0	406.0	406.0	405.8	379.4	379.5	379.6	379.5
171	382.1	382.1	382.1	382.0	406.0	406.0	406.1	405.8	379.5	379.5	379.6	379.5
181	382.1	382.2	382.1	382.0	406.1	406.1	406.1	405.8	379.5	379.6	379.6	379.6
191	382.2	382.2	382.2	382.1	406.1	406.1	406.1	405.9	379.5	379.6	379.6	379.6
201	382.2	382.2	382.2	382.1	406.1	406.1	406.1	405.9	379.6	379.6	379.6	379.6

$2m+1$	$(n, p_0) = (18, 0.7)$				$(n, p_0) = (22, 0.8)$				$(n, p_0) = (25, 0.9)$			
	0.1	0.15	0.2	0.3	0.1	0.15	0.2	0.3	0.1	0.15	0.2	0.3
51	368.5	368.8	369.2	369.4	360.9	361.1	361.3	361.4	345.2	345.6	345.5	345.0
61	372.8	371.1	370.3	370.2	360.2	361.4	361.9	362.1	345.4	346.1	346.0	345.8
71	371.2	370.5	370.5	370.6	364.8	362.9	362.5	362.6	345.8	346.5	346.3	345.8
81	370.8	370.7	370.8	370.9	362.8	362.6	362.7	362.8	345.8	346.7	346.5	346.0
91	369.9	370.8	371.0	371.1	362.9	362.8	362.9	363.0	346.4	346.9	346.7	346.1
101	370.6	371.0	371.1	371.2	362.7	362.9	363.0	363.1	347.1	347.0	346.8	346.2
111	371.0	371.1	371.2	371.3	362.7	362.9	363.0	363.2	347.2	347.1	346.8	346.3
121	371.0	371.2	371.3	371.4	363.0	363.1	363.2	363.3	347.3	347.1	346.8	346.4
131	371.1	371.3	371.4	371.5	363.0	363.1	363.2	363.3	347.3	347.2	346.9	346.4
141	371.3	371.3	371.4	371.5	363.1	363.2	363.3	363.4	347.4	347.2	347.0	346.4
151	371.3	371.4	371.5	371.6	363.1	363.2	363.3	363.4	347.4	347.2	347.0	346.5
161	371.3	371.4	371.5	371.6	363.2	363.3	363.4	363.5	347.4	347.2	347.0	346.5
171	371.4	371.4	371.5	371.6	363.2	363.3	363.4	363.5	347.4	347.2	347.0	346.5
181	371.4	371.4	371.5	371.6	363.2	363.3	363.4	363.5	347.4	347.3	347.0	346.8
191	371.4	371.5	371.6	371.7	363.2	363.3	363.4	363.5	347.4	347.3	347.1	346.8
201	371.4	371.5	371.6	371.7	363.3	363.4	363.4	363.5	347.5	347.3	347.1	346.8

Table 6.: ARL_1 values for $\lambda = 0.2, K = 2.75, n = 10, h = 0.2$ under the benchmark of the 18 Johnson distributions for different shifts using $p_0 = \{0.1, 0.5, 0, 7\}$

Cases																		
$\tau = 0.25$																		
p_0	1	2	3	4	5	6	7	8	9	10	11	12	13	14	15	16	17	18
0.1	4.95	4.95	4.95	4.95	4.97	5.00	4.95	4.96	4.97	4.99	5.03	5.08	5.11	5.07	5.06	5.12	5.22	5.30
0.2	3.00	3.00	3.00	3.00	3.00	3.01	3.00	3.00	3.00	3.01	3.02	3.04	3.09	3.04	3.03	3.06	3.11	3.16
0.5	2.00	2.00	2.00	2.00	2.00	2.00	2.00	2.00	2.00	2.00	2.00	2.00	2.00	2.00	2.00	2.00	2.00	2.01
0.7	1.00	1.02	1.09	1.16	1.23	1.29	1.16	1.09	1.08	1.20	1.30	1.37	1.21	1.15	1.14	1.32	1.44	1.50
$\tau = 0.75$																		
0.1	4.95	6.25	8.67	11.22	14.28	17.01	7.46	7.79	8.30	13.38	17.99	21.50	9.50	8.99	8.83	20.68	27.42	31.79
0.2	3.00	5.05	6.38	7.54	8.83	9.91	4.66	5.05	5.78	8.22	10.14	11.51	5.12	4.94	5.05	10.74	13.44	15.10
0.5	4.79	6.48	7.05	7.48	7.94	8.33	4.63	6.18	6.63	7.54	8.28	8.79	4.82	5.67	5.91	8.14	9.23	9.86
0.7	9.11	10.20	10.52	10.75	11.01	11.22	8.93	9.99	10.27	10.75	11.16	11.44	9.06	9.65	9.81	10.98	11.61	11.97
$\tau = 2$																		
0.1	1.12	1.42	1.58	1.72	1.88	2.01	1.32	1.48	1.55	1.80	2.03	2.20	1.42	1.48	1.50	2.06	2.42	2.64
0.2	1.57	1.84	1.95	2.03	2.13	2.21	1.79	1.90	1.94	2.08	2.22	2.33	1.87	1.91	1.92	2.23	2.45	2.59
0.5	2.96	3.14	3.20	3.24	3.29	3.33	3.12	3.18	3.20	3.27	3.33	3.38	3.18	3.19	3.19	3.34	3.43	3.49
0.7	5.06	5.19	5.22	5.25	5.28	5.31	5.18	5.21	5.23	5.27	5.31	5.34	5.22	5.22	5.22	5.31	5.37	5.40

Table 7.: Out-of-control performance for the proposed chart along with the corresponding optimal parameters for $n = 10$

case	$\tau = 0.25$	$\tau = 0.5$	$\tau = 0.75$	$\tau = 0.95$	$\tau = 1.25$	$\tau = 1.5$	$\tau = 1.75$	$\tau = 1.95$	$\tau = 2.0$
#1	(0.75,2.845)	(0.75,2.845)	(0.3,2.908)	(0.05,2.478)	(0.3,3.349)	(0.3,3.349)	(0.35,3.434)	(0.8,3.755)	(0.8,3.755)
	1	1.12	4.26	27.22	2.88	1.61	1.27	1.15	1.13
	(0.5,0)	(0.5,0.0130)	(0.25,0.018)	(0.05,0.014)	(0.05,0.233)	(0.05,0.364)	(0.05,0.457)	(0.05,0.514)	(0.05,0.526)
#2	(0.75,2.845)	(0.65,2.867)	(0.15,2.791)	(0.05,2.481)	(0.15,2.93)	(0.3,3.349)	(0.3,3.349)	(0.3,3.349)	(0.3,3.349)
	1	2.66	9.11	106.13	7.11	2.92	1.93	1.59	1.53
	(0.5,0)	(0.5,0.150)	(0.25,0.107)	(0.15,0.125)	(0.05,0.139)	(0.05,0.231)	(0.05,0.313)	(0.05,0.369)	(0.05,0.382)
#3	(0.65,2.88)	(0.4,2.89)	(0.1,2.691)	(0.05,2.483)	(0.1,2.722)	(0.25,3.244)	(0.3,3.349)	(0.3,3.349)	(0.3,3.349)
	1.05	3.07	10.99	131.57	10.33	3.97	2.43	1.92	1.83
	(0.6,0.0359)	(0.5,0.177)	(0.3,0.167)	(0.25,0.22)	(0.05,0.116)	(0.05,0.191)	(0.05,0.262)	(0.05,0.314)	(0.05,0.327)
#4	(0.7,2.876)	(0.4,2.89)	(0.1,2.695)	(0.05,2.49)	(0.15,2.829)	(0.2,2.929)	(0.3,3.349)	(0.3,3.349)	(0.3,3.349)
	1.11	3.34	12.22	145.23	12.77	5.01	2.97	2.27	2.15
	(0.6,0.057)	(0.5,0.193)	(0.35,0.221)	(0.3,0.27)	(0.1,0.176)	(0.1,0.252)	(0.05,0.228)	(0.05,0.276)	(0.05,0.287)
#5	(0.65,2.88)	(0.4,2.89)	(0.1,2.695)	(0.05,2.486)	(0.1,2.697)	(0.2,2.929)	(0.4,3.239)	(0.4,3.239)	(0.4,3.239)
	1.19	3.62	13.44	156.8	15.23	5.86	3.51	2.64	2.49
	(0.6,0.078)	(0.5,0.208)	(0.35,0.229)	(0.35,0.327)	(0.15,0.231)	(0.1,0.235)	(0.1,0.299)	(0.1,0.345)	(0.1,0.356)
#6	(0.7,2.876)	(0.35,2.889)	(0.1,2.689)	(0.05,2.486)	(0.1,2.697)	(0.2,2.88)	(0.4,3.096)	(0.4,3.239)	(0.4,3.239)
	1.25	3.81	14.3	164.51	16.93	6.47	3.92	2.93	2.75
	(0.6,0.092)	(0.55,0.268)	(0.4,0.281)	(0.35,0.328)	(0.15,0.225)	(0.15,0.296)	(0.15,0.359)	(0.1,0.327)	(0.1,0.337)
#7	(0.75,3.052)	(0.65,2.88)	(0.2,2.832)	(0.05,2.487)	(0.25,3.244)	(0.3,3.349)	(0.35,3.434)	(0.35,3.434)	(0.35,3.434)
	1.11	1.93	5.6	40.16	3.52	1.99	1.55	1.38	1.35
	(0.75,0.183)	(0.6,0.194)	(0.35,0.136)	(0.1,0.062)	(0.05,0.205)	(0.05,0.306)	(0.05,0.376)	(0.05,0.4195)	(0.05,0.429)
#8	(0.7,3.039)	(0.65,2.867)	(0.15,2.783)	(0.05,2.481)	(0.2,3.107)	(0.3,3.349)	(0.3,3.349)	(0.3,3.349)	(0.3,3.349)
	1.08	2.54	8.71	98.21	6.47	2.85	1.98	1.66	1.6
	(0.75,0.164)	(0.5,0.143)	(0.3,0.145)	(0.15,0.124)	(0.05,0.146)	(0.05,0.235)	(0.05,0.307)	(0.05,0.355)	(0.05,0.366)
#9	(0.95,2.848)	(0.4,2.89)	(0.1,2.691)	(0.05,2.489)	(0.15,2.93)	(0.3,3.349)	(0.3,3.349)	(0.3,3.349)	(0.3,3.349)
	1.1	2.86	10.01	117.81	8.27	3.39	2.22	1.81	1.74
	(0.7,0.118)	(0.5,0.162)	(0.3,0.158)	(0.2,0.175)	(0.05,0.129)	(0.05,0.210)	(0.05,0.280)	(0.05,0.329)	(0.05,0.340)
#10	(0.65,2.88)	(0.4,2.89)	(0.1,2.695)	(0.05,2.49)	(0.15,2.829)	(0.2,2.929)	(0.4,3.239)	(0.4,3.239)	(0.4,3.239)
	1.19	3.43	12.6	148.82	13.88	5.35	3.22	2.46	2.33
	(0.6,0.077)	(0.5,0.199)	(0.35,0.224)	(0.3,0.277)	(0.1,0.172)	(0.1,0.245)	(0.1,0.311)	(0.1,0.359)	(0.1,0.370)
#11	(0.65,2.88)	(0.35,2.889)	(0.1,2.689)	(0.05,2.49)	(0.1,2.697)	(0.2,2.88)	(0.4,3.096)	(0.4,3.239)	(0.4,3.239)
	1.28	3.8	14.28	164.24	17.08	6.51	3.95	2.96	2.78
	(0.6,0.097)	(0.55,0.267)	(0.4,0.280)	(0.4,0.378)	(0.15,0.224)	(0.15,0.295)	(0.15,0.358)	(0.1,0.325)	(0.1,0.335)
#12	(0.7,3.039)	(0.35,2.889)	(0.1,2.694)	(0.05,2.49)	(0.1,2.695)	(0.2,2.88)	(0.25,2.939)	(0.4,3.096)	(0.4,3.096)
	1.34	4.04	15.3	172.13	18.96	7.28	4.37	3.27	3.08
	(0.75,0.266)	(0.55,0.278)	(0.45,0.334)	(0.4,0.379)	(0.2,0.278)	(0.15,0.284)	(0.15,0.344)	(0.15,0.387)	(0.15,0.397)
#13	(0.75,3.052)	(0.65,2.88)	(0.2,2.832)	(0.05,2.487)	(0.25,3.244)	(0.3,3.349)	(0.3,3.349)	(0.3,3.349)	(0.3,3.349)
	1.13	2	6.11	48.37	3.95	2.19	1.71	1.52	1.48
	(0.75,0.194)	(0.6,0.201)	(0.35,0.148)	(0.1,0.066)	(0.05,0.191)	(0.05,0.283)	(0.05,0.346)	(0.05,0.384)	(0.05,0.393)
#14	(0.75,3.052)	(0.5,2.886)	(0.15,2.783)	(0.05,2.487)	(0.25,3.244)	(0.3,3.349)	(0.3,3.349)	(0.3,3.349)	(0.3,3.349)
	1.1	2.35	7.65	78.08	5.31	2.58	1.89	1.63	1.58
	(0.75,0.179)	(0.55,0.175)	(0.3,0.132)	(0.1,0.07)	(0.05,0.162)	(0.05,0.252)	(0.05,0.318)	(0.05,0.361)	(0.05,0.370)
#15	(0.75,3.052)	(0.5,2.886)	(0.15,2.783)	(0.05,2.487)	(0.2,3.107)	(0.3,3.349)	(0.3,3.349)	(0.3,3.349)	(0.3,3.349)
	1.09	2.46	8.21	89.88	5.91	2.74	1.96	1.67	1.62
	(0.75,0.175)	(0.55,0.185)	(0.3,0.139)	(0.1,0.07)	(0.05,0.153)	(0.05,0.241)	(0.05,0.309)	(0.05,0.3528)	(0.05,0.362)
#16	(0.75,3.052)	(0.35,2.889)	(0.1,2.694)	(0.05,2.490)	(0.1,2.695)	(0.2,2.880)	(0.4,3.096)	(0.4,3.096)	(0.4,3.096)
	1.28	3.78	14.17	162.79	17.22	6.6	4	3.01	2.84
	(0.75,0.250)	(0.55,0.2664)	(0.45,0.328)	(0.4,0.378)	(0.2,0.283)	(0.15,0.294)	(0.15,0.357)	(0.15,0.401)	(0.15,0.411)
#17	(0.7,3.039)	(0.35,2.886)	(0.1,2.694)	(0.05,2.487)	(0.1,2.696)	(0.2,2.855)	(0.3,2.940)	(0.4,3.096)	(0.4,3.096)
	1.39	4.23	16.21	178.51	20.93	8.07	4.83	3.64	3.42
	(0.75,0.279)	(0.6,0.340)	(0.45,0.338)	(0.45,0.430)	(0.25,0.329)	(0.2,0.339)	(0.2,0.398)	(0.15,0.370)	(0.15,0.380)
#18	(0.7,3.039)	(0.35,2.886)	(0.1,2.689)	(0.05,2.487)	(0.05,2.49)	(0.2,2.855)	(0.25,2.905)	(0.35,2.971)	(0.35,2.971)
	1.45	4.49	17.31	185.84	22.91	8.92	5.27	3.96	3.74
	(0.75,0.293)	(0.6,0.3495)	(0.5,0.393)	(0.45,0.430)	(0.3,0.379)	(0.2,0.330)	(0.2,0.3867)	(0.2,0.426)	(0.2,0.436)

Table 8.: Out-of-control performance for the proposed chart along with the corresponding optimal parameters for $n = 20$

case	$\tau = 0.25$	$\tau = 0.5$	$\tau = 0.75$	$\tau = 0.95$	$\tau = 1.25$	$\tau = 1.5$	$\tau = 1.75$	$\tau = 1.95$	$\tau = 2.0$
	(0.65,2.948)	(0.65,2.948)	(0.4,2.949)	(0.05,2.487)	(0.5,3.4)	(0.55,3.445)	(0.45,3.357)	(0.5,3.4)	(0.5,3.4)
#1	1 (0.35,0)	1 (0.35,0)	2.35 (0.25,0.018)	15.84 (0.05,0.014)	1.73 (0.05,0.233)	1.1 (0.05,0.364)	1.02 (0.05,0.457)	1 (0.05,0.514)	1 (0.05,0.526)
#2	(0.65,2.948)	(0.7,2.937)	(0.25,2.888)	(0.05,2.489)	(0.25,3.075)	(0.5,3.4)	(0.6,3.49)	(0.55,3.445)	(0.55,3.445)
	1 (0.35,0)	1.38 (0.4,0.0613368)	5.3 (0.25,0.107)	58.21 (0.1,0.0792381)	4.31 (0.05,0.139)	1.75 (0.05,0.231)	1.22 (0.05,0.313)	1.09 (0.05,0.369)	1.07 (0.05,0.382)
#3	(0.7,2.947)	(0.7,2.931)	(0.2,2.847)	(0.05,2.49)	(0.2,2.966)	(0.5,3.4)	(0.5,3.4)	(0.55,3.445)	(0.55,3.445)
	1 (0.35,0)	1.67 (0.45,0.130)	6.46 (0.3,0.167)	76.22 (0.2,0.177)	6.28 (0.05,0.116)	2.38 (0.05,0.191)	1.48 (0.05,0.263)	1.22 (0.05,0.314)	1.18 (0.05,0.327)
#4	(0.7,2.931)	(0.7,2.93)	(0.15,2.793)	(0.05,2.49)	(0.2,2.888)	(0.5,3.181)	(0.5,3.4)	(0.55,3.445)	(0.55,3.445)
	1 (0.45,0.01)	1.86 (0.5,0.193)	7.22 (0.35,0.221)	87.22 (0.25,0.227)	7.76 (0.1,0.176)	3 (0.1,0.252)	1.78 (0.05,0.228)	1.39 (0.05,0.276)	1.33 (0.05,0.287)
#5	(0.75,2.927)	(0.7,2.93)	(0.15,2.792)	(0.05,2.489)	(0.2,2.867)	(0.3,3.004)	(0.55,3.21)	(0.55,3.21)	(0.55,3.21)
	1 (0.5,0.034)	2.06 (0.5,0.208)	7.9 (0.4,0.276)	96.79 (0.3,0.278)	9.22 (0.15,0.231)	3.54 (0.1,0.235)	2.07 (0.1,0.299)	1.59 (0.1,0.345)	1.52 (0.1,0.356)
#6	(0.75,2.927)	(0.7,2.931)	(0.15,2.792)	(0.05,2.489)	(0.15,2.802)	(0.3,2.946)	(0.55,3.21)	(0.55,3.21)	(0.55,3.21)
	1.01 (0.5,0.045)	2.19 (0.55,0.268)	8.4 (0.4,0.281)	103.28 (0.35,0.328)	10.28 (0.15,0.225)	3.92 (0.15,0.296)	2.32 (0.1,0.282)	1.75 (0.1,0.327)	1.66 (0.1,0.337)
#7	(0.85,2.969)	(0.7,2.937)	(0.35,2.92)	(0.05,2.487)	(0.5,3.4)	(0.55,3.445)	(0.55,3.445)	(0.5,3.4)	(0.5,3.4)
	1 (0.7,0.146)	1.19 (0.6,0.194)	3.25 (0.35,0.136)	22.66 (0.05,0.022)	2.1 (0.05,0.205)	1.25 (0.05,0.306)	1.08 (0.05,0.376)	1.04 (0.05,0.419)	1.03 (0.05,0.429)
#8	(0.75,2.927)	(0.75,2.927)	(0.25,2.888)	(0.05,2.489)	(0.25,3.075)	(0.5,3.4)	(0.55,3.445)	(0.5,3.4)	(0.5,3.4)
	1 (0.5,0.034)	1.38 (0.5,0.143)	5.09 (0.25,0.103)	53.13 (0.1,0.078)	3.94 (0.05,0.146)	1.71 (0.05,0.235)	1.25 (0.05,0.307)	1.12 (0.05,0.355)	1.1 (0.05,0.366)
#9	(0.75,2.927)	(0.75,2.927)	(0.2,2.847)	(0.05,2.49)	(0.2,2.966)	(0.5,3.4)	(0.5,3.4)	(0.6,3.49)	(0.5,3.4)
	1 (0.5,0.030)	1.53 (0.5,0.162)	5.84 (0.3,0.158)	66.68 (0.15,0.127)	5.02 (0.05,0.129)	2.03 (0.05,0.210)	1.37 (0.05,0.280)	1.17 (0.05,0.329)	1.15 (0.05,0.340)
#10	(0.7,2.931)	(0.7,2.93)	(0.15,2.793)	(0.05,2.489)	(0.2,2.867)	(0.3,3.004)	(0.55,3.21)	(0.55,3.445)	(0.55,3.445)
	1 (0.55,0.054)	1.93 (0.5,0.1991)	7.44 (0.35,0.224)	90.67 (0.3,0.277)	8.4 (0.15,0.236)	3.23 (0.1,0.245)	1.91 (0.1,0.311)	1.49 (0.05,0.260)	1.42 (0.05,0.270)
#11	(0.7,2.931)	(0.7,2.931)	(0.15,2.792)	(0.05,2.489)	(0.15,2.799)	(0.3,2.946)	(0.45,3.038)	(0.55,3.21)	(0.55,3.21)
	1.01 (0.55,0.071)	2.19 (0.55,0.267)	8.38 (0.4,0.280)	103.09 (0.35,0.328)	10.32 (0.2,0.284)	3.94 (0.15,0.295)	2.34 (0.15,0.358)	1.77 (0.1,0.325)	1.67 (0.1,0.335)
#12	(0.75,2.929)	(0.65,2.939)	(0.15,2.792)	(0.05,2.489)	(0.15,2.799)	(0.35,2.953)	(0.45,3.038)	(0.65,3.038)	(0.65,3.038)
	1.02 (0.55,0.083)	2.34 (0.6,0.332)	9.02 (0.4,0.286)	110.36 (0.4,0.379)	11.48 (0.2,0.278)	4.39 (0.2,0.350)	2.58 (0.15,0.344)	1.97 (0.2,0.453)	1.86 (0.2,0.463)
#13	(0.8,3.001)	(0.7,2.937)	(0.35,2.92)	(0.05,2.489)	(0.5,3.4)	(0.55,3.445)	(0.55,3.445)	(0.5,3.4)	(0.5,3.4)
	1 (0.75,0.194)	1.22 (0.6,0.201)	3.56 (0.35,0.148)	27.16 (0.1,0.066)	2.37 (0.05,0.191)	1.35 (0.05,0.283)	1.13 (0.05,0.346)	1.07 (0.05,0.384)	1.06 (0.05,0.393)
#14	(0.6,2.959)	(0.75,2.929)	(0.3,2.911)	(0.05,2.489)	(0.45,3.357)	(0.5,3.4)	(0.55,3.445)	(0.6,3.49)	(0.5,3.4)
	1 (0.7,0.1459)	1.3 (0.55,0.175)	4.46 (0.3,0.132)	42.1 (0.1,0.074)	3.24 (0.05,0.162)	1.56 (0.05,0.252)	1.21 (0.05,0.318)	1.1 (0.05,0.361)	1.09 (0.05,0.370)
#15	(0.65,2.948)	(0.75,2.929)	(0.25,2.885)	(0.05,2.489)	(0.25,3.075)	(0.5,3.4)	(0.55,3.445)	(0.55,3.445)	(0.55,3.445)
	1 (0.65,0.111)	1.36 (0.55,0.185)	4.81 (0.3,0.139)	48.16 (0.1,0.076)	3.62 (0.05,0.153)	1.65 (0.05,0.241)	1.24 (0.05,0.309)	1.12 (0.05,0.3529)	1.1 (0.05,0.362)
#16	(0.75,2.929)	(0.65,2.939)	(0.15,2.792)	(0.05,2.489)	(0.15,2.799)	(0.3,2.946)	(0.45,3.038)	(0.55,3.21)	(0.55,3.21)
	1.02 (0.55,0.083)	2.16 (0.6,0.32)	8.34 (0.4,0.280)	102.38 (0.35,0.328)	10.4 (0.2,0.283)	4 (0.15,0.294)	2.37 (0.15,0.357)	1.8 (0.1,0.321)	1.71 (0.1,0.331)
#17	(0.7,2.937)	(0.65,2.939)	(0.15,2.792)	(0.05,2.489)	(0.1,2.697)	(0.3,2.927)	(0.45,3.038)	(0.6,3.028)	(0.6,3.028)
	1.04 (0.6,0.130)	2.47 (0.6,0.340)	9.57 (0.45,0.338)	116.03 (0.4,0.380)	12.65 (0.25,0.329)	4.86 (0.2,0.339)	2.89 (0.15,0.329)	2.14 (0.2,0.440)	2.02 (0.2,0.450)
#18	(0.95,2.876)	(0.45,2.935)	(0.15,2.792)	(0.05,2.489)	(0.1,2.698)	(0.3,2.918)	(0.4,2.971)	(0.6,3.028)	(0.6,3.028)
	1.05 (0.65,0.181)	2.65 (0.6,0.349)	10.25 (0.45,0.343)	123.14 (0.4,0.381)	13.75 (0.3,0.379)	5.33 (0.25,0.391)	3.16 (0.2,0.386)	2.34 (0.2,0.426)	2.2 (0.2,0.436)

Table 9.: Out-of-control performance of the D-SN-C EWMA chart versus several parametric control charts when the underlying distribution is the Normal for $n = \{5, 20, 30\}$

τ	Zhang's R Chart			Zhang's S Chart			Khoo and Lim's R Chart			D-SN-C EWMA Chart		
	$n = 5$	$n = 10$	$n = 20$	$n = 5$	$n = 10$	$n = 20$	$n = 5$	$n = 10$	$n = 20$	$n = 5$	$n = 10$	$n = 20$
0.1	1.04	1.00	1.00	1.03	1.00	1.00	1.14	1.00	1.00	(0.7,2.951) 1 (0.7,0)	(0.75,2.846) 1 (0.5,0)	(0.65,2.948) 1 (0.35,0)
0.2	2.66	1.00	1.00	2.62	1.00	1.00	4.22	1.01	1.00	(0.65,2.958) 1.27 (0.7,0.05)	(0.65,2.881) 1 (0.6,0.008)	(0.65,2.948) 1 (0.35,0)
0.3	8.58	1.23	1.00	8.45	1.14	1.00	15.13	1.46	1.00	(0.6,2.958) 2.14 (0.7,0.199)	(0.65,2.881) 1.2 (0.6,0.080)	(0.75,2.935) 1 (0.4,0.005)
0.4	23.08	2.53	1.08	22.62	2.27	1.01	41.19	3.57	1.15	(0.5,2.787) 3.31 (0.5,0.091)	(0.7,2.861) 1.85 (0.5,0.091)	(0.75,2.929) 1.11 (0.45,0.058)
0.5	51.96	6.75	1.71	51.79	6.14	1.34	90.55	10.45	2.04	(0.3,2.827) 5.24 (0.55,0.231)	(0.4,2.886) 3.06 (0.5,0.177)	(0.7,2.932) 1.67 (0.45,0.130)
0.6	101.99	19.12	4.20	103.07	17.71	3.10	173.87	30.56	5.55	(0.15,2.764) 8.28 (0.45,0.208)	(0.3,2.892) 4.88 (0.45,0.2080)	(0.45,2.935) 2.82 (0.4,0.160)
0.7	181.22	52.19	13.60	185.49	49.66	10.58	288.14	79.70	18.89	(0.1,2.684) 13.89 (0.35,0.181)	(0.05,2.123) 7.83 (0.35,0.181)	(0.25,2.884) 4.73 (0.35,0.181)
0.8	301.02	134.53	50.44	307.97	129.11	42.94	433.69	189.02	68.61	(0.05,2.482) 26.12 (0.3,0.195)	(0.05,2.123) 13.34 (0.35,0.242)	(0.15,2.797) 9.27 (0.25,0.150)
0.9	423.90	308.45	188.04	444.64	300.21	174.67	520.23	373.87	232.12	(0.05,2.482) 80.41 (0.3,0.249)	(0.05,2.123) 34.88 (0.35,0.299)	(0.05,2.491) 26.21 (0.2,0.154)
1.05	266.38	258.73	248.50	263.01	225.27	187.23	268.00	260.36	250.36	(0.05,2.467) 124.63 (0.05,0.061)	(0.05,2.207) 81.34 (0.25,0.273)	(0.05,2.49) 64.72 (0.1,0.117)
1.1	172.68	148.12	127.59	157.38	120.29	78.82	182.01	160.40	139.97	(0.05,2.467) 57.26 (0.05,0.074)	(0.05,2.207) 36.6 (0.25,0.295)	(0.1,2.701) 24.47 (0.1,0.134)
1.15	110.96	87.26	66.21	99.95	63.97	35.54	123.02	98.38	76.27	(0.05,2.467) 33.61 (0.05,0.088)	(0.1,2.738) 21.65 (0.05,0.088)	(0.15,2.85) 13.36 (0.05,0.088)
1.2	73.80	52.27	37.91	64.13	12.57	18.32	84.63	62.24	44.01	(0.05,2.467) 22.88 (0.05,0.1023985)	(0.1,2.738) 14.22 (0.05,0.102)	(0.15,2.85) 8.66 (0.05,0.102)
1.3	35.50	22.35	14.32	30.48	14.99	6.72	44.69	28.29	17.77	(0.1,2.84) 12.99 (0.05,0.1316303)	(0.15,2.935) 8.03 (0.05,0.131)	(0.2,2.966) 4.86 (0.05,0.131)
1.4	19.61	11.53	7.11	16.85	7.76	3.43	25.91	15.27	8.86	(0.1,2.84) 8.87 (0.05,0.16150788)	(0.25,3.255) 5.39 (0.05,0.161)	(0.45,3.358) 3.27 (0.05,0.161)
1.5	12.23	6.89	4.17	10.49	4.74	2.20	16.70	9.27	5.20	(0.15,3.105) 6.65 (0.05,0.19131831)	(0.25,3.255) 3.99 (0.05,0.191)	(0.5,3.4) 2.38 (0.05,0.191)
1.6	8.30	4.63	2.78	7.20	3.26	1.64	11.89	6.26	3.49	(0.2,3.288) 5.28 (0.05,0.2205657)	(0.3,3.356) 3.16 (0.05,0.220)	(0.5,3.4) 1.88 (0.05,0.220)
1.8	4.70	2.62	1.68	1.80	2.01	1.20	7.00	3.60	2.07	(0.25,3.424) 3.75 (0.05,0.27619046)	(0.3,3.356) 2.28 (0.05,0.276)	(0.55,3.445) 1.39 (0.05,0.276)
2	3.17	1.84	1.28	2.87	1.51	1.07	4.85	2.49	1.53	(0.25,3.424) 2.95 (0.05,0.32707178)	(0.3,3.356) 1.83 (0.05,0.327)	(0.55,3.445) 1.18 (0.05,0.327)
3	1.41	1.07	1.00	1.35	1.03	1.00	2.03	1.25	1.04	(0.3,3.536) 1.64 (0.05,0.51352518)	(0.8,3.756) 1.15 (0.05,0.513)	(0.5,3.4) 1 (0.05,0.513)

Table 10.: Performance comparisons between the Shewhart and EWMA Sign charts for dispersion when $n = 20$ using (13)

case	$\tau = 0.5$	$\tau = 0.75$	$\tau = 0.95$	$\tau = 1.25$	$\tau = 1.5$	$\tau = 1.75$	$\tau = 1.95$	$\tau = 2.0$
1	32.90	-80.88	-77.24	-70.16	-45.00	-25.53	-21.05	-15.33
2	3.51	-79.62	-65.92	-64.73	-40.19	-18.29	-14.44	-6.71
3	-14.29	-79.92	-59.70	-64.97	-43.44	-18.15	-10.04	1.03
4	39.46	-79.93	-79.22	-72.06	-47.43	-27.41	-22.01	-15.97
5	-0.41	-79.28	-64.57	-64.06	-40.54	-16.48	-12.69	-4.65
6	-22.19	-80.09	-57.02	-66.05	-46.22	-21.05	-11.97	-0.46
7	37.93	-79.43	-81.17	-73.16	-48.49	-28.64	-22.84	-16.44
8	-29.65	-80.37	-54.84	-67.48	-49.64	-25.30	-15.65	-3.27
9	-35.89	-79.89	-52.17	-68.64	-52.85	-30.71	-21.13	-8.66

Table 11.: Performance comparisons in terms of the ARL_1 values between the AC-EWMA and D-SN-C EWMA charts for when $n = 10$

	D-SN-C EWMA	AC-EWMA	D-SN-C EWMA	AC-EWMA
τ	Normal		Double Exponential	
1	370.4	370.50	370.4	370.50
1.2	17.64	46.52	30.69	18.50
1.4	6.62	12.06	10.62	17.10
1.6	4.25	7.60	6.30	16.10
1.8	3.28	5.42	4.61	9.80
2	2.77	4.37	3.74	5.30
2.2	2.47	3.76	3.22	4.80
2.4	2.26	3.38	2.87	4.40
2.6	2.12	3.13	2.63	3.70
2.8	2.01	2.97	2.45	3.40
3	1.93	2.85	2.31	3.10

Table 12.: Values of SD_t , SD_t^* , Z_t^* of each subgroups for the two scenarios

Subgroup	scenario plotted in Figure 4			scenario plotted in Figure 5		
	SD_t	SD_t^*	Z_t^*	SD_t	SD_t^*	Z_t^*
1	-5	-5.023	-4.631	-3	-3.148	-0.787
2	-5	-4.784	-4.669	-1	-0.777	-0.785
3	-5	-4.816	-4.706	3	2.522	0.042
4	-3	-2.952	-4.267	1	1.375	0.375
5	-5	-5.137	-4.485	1	0.747	0.468
6	-5	-5.047	-4.625	1	1.078	0.621
7	-5	-5.130	-4.752	5	5.146	1.752
8	-5	-4.806	-4.765	-3	-2.942	0.578
9	-5	-5.109	-4.851	1	0.944	0.670
10	-3	-3.271	-4.456	3	3.107	1.279
11	-5	-4.958	-4.581	1	1.182	1.255
12	-5	-4.820	-4.641	-3	-3.028	0.184
13	-3	-2.773	-4.174	3	3.020	0.893
14	-5	-5.028	-4.388	1	1.037	0.929
15	-3	-2.857	-4.005	5	5.050	1.959
16	-5	-5.274	-4.322	3	3.345	2.306
17	-5	-5.194	-4.540	1	0.893	1.952
18	-5	-5.212	-4.708	3	2.997	2.214
19	-5	-4.823	-4.737	-1	-1.235	1.351
20	-5	-4.951	-4.790	1	0.448	1.126
21	-1	-0.563	-3.733	-3	-3.037	0.085
22	-3	-3.125	-3.581	-5	-4.742	-1.122
23	-3	-3.179	-3.481	1	1.081	-0.571
24	-3	-2.744	-3.296	-5	-5.418	-1.783
25	-1	-0.938	-2.707	-5	-4.948	-2.574
26	-1	-0.996	-2.279	-5	-5.247	-3.242
27	1	0.907	-1.483	-1	-1.121	-2.712
28	-1	-0.683	-1.283	-5	-5.285	-3.355
29	-3	-3.576	-1.856	-3	-3.095	-3.290
30	1	1.194	-1.093	-3	-3.178	-3.262